Cosmological Consequences of Some New Versions of Dark Energy Models

By

Sabir Hussain

CIIT/FA17-RMT-046/LHR

MS Thesis

In

Mathematics

COMSATS University Islamabad

Lahore Campus

Spring, 2019

COMSATS University Islamabad
Lahore Campus

Cosmological Consequences of Some New Versions of Dark Energy Models

A Thesis Presented to

COMSATS University Islamabad, Lahore Campus.

In partial fulfillment

of the requirement for the degree of

MS (Master of Science in Mathematics)

By

Sabir Hussain

CIIT/FA17-RMT-046/LHR

Spring, 2019

Cosmological Consequences of Some New Versions of Dark Energy Models

A Post Graduate Thesis submitted to the Department of Mathematics as partial fulfillment of the requirement for the award of Degree of M.S (Master of Science in Mathematics).

Name	Registration Number
Sabir Hussain	CIIT/FA17-RMT-046/LHR

Supervisor

Dr. Abdul Jawad

Assistant Professor, Department of Mathematics

COMSATS University Islamabad, Lahore Campus

June, 2019

Final Approval

This thesis titled

Cosmological Consequences of Some New Versions of Dark Energy Models

By

SABIR HUSSAIN

CIIT/FA17-RMT-046/LHR

Has been approved

For the COMSATS University Islamabad (CUI), Lahore Campus.

External Examiner:____

Dr. Rizwana Kausar

CAMS, UCP Business School, University of Central Punjab, Lahore

Supervisor:____

Dr. Abdul Jawad

Department of Mathematics, (CUI) Lahore Campus

HoD:____

Dr. Sarfraz Ahmad

Department of Mathematics, (CUI) Lahore Campus

Declaration

I, **Sabir Hussain** with registration number **CIIT/FA17-RMT-046/LHR** hereby declare that I have produced the work presented in this thesis, during the scheduled period of study. I also declare that I have not taken any material from any source except referred to wherever due, that amount of plagiarism is within acceptable range. If a violation of HEC rules on research has occurred in this thesis, I shall be liable to punishable action under the plagiarism rules of the HEC.

Date: ______________

Sabir Hussain

CIIT/FA17-RMT-046/LHR

Certificate

It is certified that **Sabir Hussain** with **CIIT/FA17-RMT-046/LHR** has carried out all the work related to this thesis under my supervision at the Department of Mathematics, COMSATS Institute of Information Technology, Lahore campus and the work fulfills the requirement for award of MS degree.

Date: __________________

Supervisor:

Dr. Abdul Jawad
Assistant Professor

Head of Department:

Dr. Sarfraz Ahmad
Associate Professor
Department of Mathematics

DEDICATED TO

My loving Daughter
Laiba Sabir

Table of Contents

List of Figures

Acknowledgements

For the sake of **Allah** most beneficent generally benevolent. By the beauty of **Allah** Almighty **whose** assistance and direction was felt at each progression and breath amid the planning of this thesis. My significant appreciation to **Hazrat Muhammad (PBUH)** Who is everlastingly a track of direction and learning for mankind in general.

I express my true thankfulness to my profoundly learned, committed supervisor **Dr. Abdul Jawad** and **Dr. Shamaila Rani** for their assistance as well as their ceaseless help, profitable remarks, advices and proposals for me. I am thankful to all my teachers, in particular, Prof. Dr. Aqeel Ahmad Khan, Mr. Saqib khan Mr. Iftikhar Ahmad and Mr. Haseeb Ahmad for their noble help and encouragement during my stay here. I also admire the help of HoD of Mathematics Department, Dr. Sarfraz Ahmad and other faculty members. I would also like to express my warm and sincere thanks to friends, especially, Mr. Muhammad Akmal, Mr. Farooq Abid, Mr. Dilawar Ali, Mr. Wakeel Ahmad, Mr. Adnan Aashiq, Mr. Sana Ullah Lashari and Mr. Hidayat Ullah for their moral support in various aspects and friendly cooperation during my studies.

This acknowledgement will remain incomplete if I do not say a few words about my parents especially for my **father** for his lot of support and prayers, which will always remain behind me **In Sha Allah**. I would like to express my gratitude towards my family specially for my brother **Muhammad Arif** for the encouragement and lot of support which help me in completion of this thesis. Many special thanks are due to my sisters whose prayers have always been with me. This acknowledgement shall remain inconclusive without mentioning my loveable wife whose love, respects and prayers have always been with me. This thesis become a reality with the kind support and help of many individuals, my colleagues and friends. I would like to thanks all of them.

Lahore **Sabir Hussain**
Spring, 2019

Abstract

It is observed that the universe expanding with repulsive force. Dark energy is an unknown force and responsible for current cosmic acceleration. Generally, in order to find the best-fit model to discuss the cosmic acceleration and dark energy phenomenon, there are two directions that are dynamical dark energy models and modified theories of gravity. One of the dynamical model is holographic dark energy which is also modified in different forms such as modified, generalized, Tsallis, Renyi, Sharma-Mittal holographic dark energy models, etc. The modified theories include fractal cosmology, Dvali-Gabadadze-Porrati braneworld, second Randall-Sundrum braneworld, loop quantum cosmology, dynamical Chern-Simons gravity, $f(R)$, $f(T)$, $f(R,T)$ theories of gravity etc. Taking some of these models and theories, researchers established different cosmological parameters.

In this thesis, we use Tsallis holographic dark energy model with generalized ghost pilgrim dark energy as infra-red cutoff for modified theories of gravity such as cyclic universe, Dvali-Gabadadze-Porrati braneworld, Randal-Sundrum II braneworld and dynamical Chern-Simons theory in the flat Friedmann-Robertson-Walker universe. In these directions, we study some cosmological parameters like equation of state, deceleration parameter, squared sound speed and Om (combination of Hubble and cosmos redshift parameter) parameter. We also establish some cosmic planes such as $\omega - \omega'$ and $r - s$ on the basis of present day observational data.

CHAPTER 1
Introduction

The researchers have been thinking about the beginning of life and the universe for thousands of years. Each culture has explained their own creation story that how did it come into being. Recently, with the help of modern telescopes and computer modeling, we are accepting and understanding the structure, evolution and origin of the universe to be very closed. However, many astronomers have been trying to explain the universe and its facts through different observational schemes. The developments of modern theory of general relativity described the behavior of gravity of the universe and provided the understanding about the subject of cosmology. Thus, the cosmology deals with the study of the universe structure, its origin and evolution. Recent observational evidences from supernovae type Ia [1]-[4], astrophysical cosmic microwave background anisotropies [5]-[7] and the large scale structure [8]-[11] motivated that the universe is undergoing an exponential expansion at an increasing rate.

The accelerated expansion means velocity of the galaxies move back from the observer is increasing with time in a continuous manner. This unexpected result shows the expansion of the universe with accelerating rate. The universe is expanding due to an unknown source which is called dark energy (DE) having negative pressure [12]. According to some cosmological observations, the 73% of the total energy of the universe has been associated with DE. From universe expansion, we realized that the DE does not follow local gravitational effects but has global effects on the universe. The first and simple candidate of DE is the cosmological constant which bears some problems afterwards [13, 14]. There are two different approaches to deal with DE scenario. One is the modified/alternative theories of gravity and other is the dynamical DE models. The theories consist on various modifications of Ricci scalar and torsion scalar in the action of general relativity and teleparallel gravity, or massive theories of gravity and higher-dimensional theories. There are many DE models proposed so far some of them are quintessence scenario, phantom (ghost) field K-essence, Chaplygin gas, agegraphic DE models, etc [15]-[26]. Also, the quantum theory of gravity gives motivation to solve the DE problem has arisen a lot of attentions.

Dark matter (DM) is another important ingredient of the universe contents which exists in the form of baryonic and non-baryonic matter. In the whole universe nearly 23% of energy budget is associated with non-baryonic DM while 4% is to the normal baryonic matter. The DM is detected by the emission of photon because stars emit light in the form of IR and ultraviolet spectrum. Some Cosmologist observed that non-baryonic DM is not detected directly from the universe because it does not absorb, emit or reflect light. In the universe, the galaxies exist in the form of cluster. For maintaining velocities of the galaxies and holding cluster together, it must take control greater amount the baryonic DM, because visible candidates of galaxies like stars and gases do not possess enough gravitational force of attraction. We can detect DM by calculating orbital speed of the stars in galaxies.

Nowadays, large extra dimensional theories have attained much attention for describing the accelerated expansion of the universe which inspired by string and super string theories. Specifically, we are able to know that our universe is brane embedded with higher dimensional bulk. In this series of theories, the effective Friedmann equation helps for current evolution of the universe. One of the most popular picture in the braneworld scenarios has been developed by Dvali-Gabadadze-Porrati (DGP). This braneworld scenario helps to leak the gravity from lower dimension to higher dimension which nominated as main source of accelerated expansion. There are two main branches of the solution has been characterized in DGP braneworld scenario which is $\epsilon = \pm 1$ [27, 28]. In self-accelerated ($\epsilon = +1$) branch, DE phenomena works for accelerating phase of the universe without invoking any exotic fluid [27]. Normal branch ($\epsilon = -1$) explored for HDE scenario, where it predicted that the universe is in accelerating phase in the presence of DE component [29].

The Randall-Sundrum II (RS-II) is another framework of braneworlds model [30], which also derived from the string theory. This braneworld model investigated about the conversion of our four dimensional world in a higher-dimensional space time. RS II braneworld model has collected the motivation of four dimensional bulk with positive tension and five-dimensional brane space time having negative cosmological constant. This matter gravity can originate through the bulk space time while the matter fields are enclosed on the brane. It is obvious that a mass on the brane produced the weak gravitational field which follows the usual 4-dimensional

Newton law containing a corrected large distance from the source [30]-[34], however these extra-dimensional bulk increases infinitely in this model. Hence, it means that this fact contain many difficulties for investigation this scenario from 4-dimensional model. Although, our observations remains on the effect of strong gravity, in which the effect of strong gravity becomes essential that the formation of an objects is possible after a strong gravitational collapse on the brane.

In cyclic framework, we are able to know that our universe is continuously expanding and contracting. The motivation of an oscillating universe firstly proposed by Tolman [35]. In modern cosmology, Steinhardt and Turok [36]-[40] investigated a cyclic model of the universe with the replacement of inflation framework. Steinhardt et al. [38], proposed a new version of cyclic model in which the cyclicity of the universe is realized in the light of two different branes. Although, this new cyclic model suffers from two main problems including the black hole and entropy problems [41]-[43]. It is useful to note that these cyclic universe problems can be solved by considering some consequences of phantom DE [41, 42]. At the beginning, the cyclic universe is promoted by an enormously high energy density and we realized that if the phantom dark energy increases in a finite time more than our expectation then it shows the end point of a cycle [43, 44]. As a result of this scenario, some expectations has arisen that the high energy physics induces some modifications to the Friedmann equation. Recently, for such case some modifications have been explored such as loop quantum cosmology [45, 46].

Chern-Simons theory firstly proposed by two cosmologist Shiing-shen Chern and James Simons. After this research, Edward Witten named this theory is a 3-dimensional topological quantum field theory of Schwarz type. However, there are two theories of Chern-Simons (CS) such as dynamical and non dynamical which are described independently. In the framework of non dynamical CS theory, a kinetic term ignored for the external field and a functional form of the external field is chosen by hand. But in the term of dynamical CS theories, the external scalar function is investigated as dynamical field [47] with the choice of kinetic term for the CS scalar field. In this case, the functional form of the CS scalar field is no longer given by hand and must be obtained by solving the dynamical field equations.

Dynamical CS modified gravity is one of the alternative theories of general relativity [48]-[50]. We get also CS modified gravity specific from the string theory [51]. This modified theory of gravity exhibits the contravention of parallel regularity in Einstein−Hilbert action considering as of the addition of the Pontryagin density. In addition, this modification consists of Pontryagin density which is a topological term in 4 dimensions where coupling constant proposed to a scaler field [52, 53]. We get dynamical CS results by putting Einstein- Hilbert term with the combination of dynamical scaler and Pontryagin energy density plus action of scaler field. The explanation of dynamical CS modified gravity is shown in Alexander and Yunes [54]. Moreover, many cosmological results have been proposed by taking distinct HDE models with dynamical CS modified gravity [55]-[57].

The idea of holographic DE (HDE) came from the holographic principle [58] which states that all information about a physical system in some region of space is encoded in its boundary surface but not in its volume. After this, Cohen et al. [59] proposed a model between ultraviolet and infra-red (IR) cutoffs. According to this model, the vacuum energy of a system should not be exceeded the mass of the black hole ($L^3_{\rho_D} \leq L_{M_p^2}$, L is represent as size, ρ_D is a HDE density and M_p^2 is a reduced Planck mass). Moreover, Hawking proposed another theory which tells that the horizon area of black hole cannot be decrease with time. According to Bekenstein [60]-[62] entropy relations, the black hole horizon area is inversely proportional to its entropy. After that, this relation was proved by Hawking [63] which is given as $S_{BH} = A/4G$. Here A represents the horizon area given as $A = 4\pi r^2$. Later, this black hole entropy recognized as the holographic principle [64, 65]. Hence the energy density of HDE model is defined as

$$\rho_D = 3c^2 M_p^2 L^{-2}, \tag{1.0.1}$$

where c^2 and L are constant and IR cutoff respectively and $M_p^2 = 1/8\pi G$ is the reduced Planck mass [66, 67].

In addition, Tsallis and Citro [68] proposed a relation between entropy and horizon area of the black hole as $S_\delta = \gamma A^\delta$, where δ is a non-additivity parameter and γ represents an unknown constant [68]. Based on the holographic principle and IR cutoffs, Cohen et al. [59] derived some entropy relations ($L^3\Lambda^3 \leq S^{3/4}, \Lambda^4 \leq \gamma(4\pi)^\delta L^{2\delta-4}$, where Λ^4 denotes the vacuum energy density). Combining above entropy inequalities with HDE density, the density of Tsallis HDE model can be proposed as

$$\rho_D = BL^{2\delta-4}, \tag{1.0.2}$$

here B is an arbitrary constant [69]-[71]. Recently, using Tsallis generalized entropy [68] and HDE scenario, a new HDE model has been proposed. For this purpose, a generalized ghost pilgrim dark energy (PDE) plays an important role as IR cutoff, is given in the following form

$$\rho_D = B(\alpha H + \beta H^2)^{4-2\delta}. \tag{1.0.3}$$

Here α and β are the arbitrary constants, $H = \frac{\dot{a}}{a}$ is the Hubble parameter and $B = (3c^2 M_p^{4-u})^{1/u}$ (u for pilgrim dark energy parameter).

Recently, the HDE framework such as cyclic, DGP and RS II braneworlds obtained by using HDE idea and Bekenstein entropy with different IR cutoffs [68]-[79]. In case of non-linear mutual interacting scenario, the generalized entropy such as Tsallis HDE model with combining Hubble horizon as IR cutoff used to evaluate some different cosmic implications [80]. There is also shown the unstable Tsallis HDE model by taking non-linear interacting case [80]. Tsallis HDE model in the frameworks of the cyclic, DGP and RS II with respect to Hubble horizon as IR cutoff used to shown that during the cosmic evolution the HDE models are not always stable [81]. In this work, we adopt different DE models and investigate their behavior through different cosmological parameters and planes in flat universe. We have extended this work by choosing Tsallis HDE with generalized ghost PDE as IR cutoff in the flat universe models. This thesis is organized as follows:

- In **chapter 2**, we provide the detail and mathematical formulation related to basic concepts and DE models.

- In **chapter 3**, the Tsallis HDE with generalized ghost PDE as IR cutoff are discussed with cosmological parameters such as Hubble parameter H, EoS parameter ω and deceleration parameter q. We also discuss cosmological planes such as $\omega - \omega'$ and $r - s$ plane in the framework of cyclic universe for flat universe.

- In **chapter 4**, the Tsallis HDE with generalized ghost PDE as IR cutoff are discussed with cosmological parameters such as Hubble parameter H, EoS parameter ω and deceleration parameter q. We also discuss cosmological planes such as $\omega-\omega'$ and $r-s$ plane in the framework of DGP braneworld and RS II braneworld for flat universe.

- In **chapter 5**, the Tsallis HDE with generalized ghost PDE as IR cutoff are discussed with cosmological parameters such as Hubble parameter H, EoS parameter ω and deceleration parameter q. We also discuss cosmological planes such as $\omega - \omega'$ and $r - s$ plane in the framework of dynamical CS gravity for flat universe.

- In last chapter, we summarize the discussion.

Chapter 2
Preliminaries

In this chapter, we furnish some basic ingredients of modern cosmology for understanding this thesis.

2.1 General Theory of Relativity

Einstein "General Theory of Relativity" suggested in 1916, which is known as theory of gravity and motivations come from his earlier special theory of relativity which has proposed in 1905. Before this, In 1687, Newton gave laws of gravitation also known as universal laws of gravitation. Newton suggests that all bodies having mass attracts each other over space. Although, this Newton idea has been replaced with the theory of general relativity. General theory of relativity states that the acceleration and gravity are identical to each other and explain the principle of equivalence. Einstein suggests that the gravity worked as a property of geometry of the space time. As he make sense by working out on the equations for his general theory of relativity, he sympathized that massive objects make caused a distortion in space time. It predicts the existence of the black holes in our universe, time delation, length contraction, curvature of the space time and an expanding universe.

2.2 Cosmological Principle and FRW Universe

In modern cosmology, the universe is a homogenous and isotropic on the large scale structure is called cosmological principle. This means all the observers and cosmologist see the universe in isotropic form near them. This principle states that the all cosmic properties of the universe is same at same cosmic time. The modern Copernican principle describes the information about isotopical only detectable phase of the universe while the cosmological principle give predictions about detectable and non detectable eras of the universe. FRW space time satisfies all the properties of the universe as spatially isotropic and homogenous which is given by

$$ds^2 = -dt^2 + a(t)^2\left(\frac{dr^2}{1-kr^2} + r^2(d\theta^2 + \sin^2(\theta)d\phi^2)\right). \qquad (2.2.1)$$

This metric is combined with two characteristic parameters such as spatial or constant curvature k and scale factor $a(t)$. With the help of scale factor we see expansion of the universe.

The spatial curvature k explains three different universe models. If the curvature $k = 0$ then the space is considered as perfectly flat, if $k = +1$, represents the closed model of the universe where surface is a sphere. While, $k = -1$, the curvature corresponds to open model of the universe where surface remains as saddle form. The energy-momentum tensor is quantity of the universe which can distribute the matter and energy of the universe. We consider perfect fluid for the matter contents FRW universe as

$$T_{ab} = (p + \rho)u_a u_b + g_{ab}p. \qquad (2.2.2)$$

Here $u_a = (1, 0, 0, 0)$ is represents the co-moving four velocity of the perfect fluid, p and ρ express as energy density and energy pressure of the fluid, respectively. The best fit field equation is

$$H^2 = \frac{8\pi G}{3}\rho - \frac{k}{a^2}, \qquad (2.2.3)$$

where $H = H(t) = \frac{\dot{a}}{a}$ is a Hubble parameter which distinguish the recessional velocities of galaxies. In addition, we found that many researcher mostly favor the flat universe. However, there are a lot of controversy through observational data about the existence of small fraction of spatial fractional density in the total fractional energy ingredients of the universe. Recent observations state that, if the number of e-folding are small then mostly the universe behaves like non flat [96].

2.3 Cosmology

The word cosmology derived from the "cosmos" Greek word. Our universe is a combination of matter which exists in two forms named as visible and invisible matter. Only 5% parts of the universe contain visible matter which is given in the form of galaxies, planets, stars etc. The invisible matter contain 23% parts of the total universe and reaming part of the universe exists with a repulsive force which compels to accelerate our universe. Hence, our universe is expanding and this expanding universe study is called cosmology. According to astronomy, the cosmology involves the structure, origin and evolution of the universe from the Big Bang to today. However, we deals the nature, structure, physical and geometrical aspects of the universe with the help of this astronomy branch. But according to NASA research, cosmology is a scientific study of the large scale structure properties of the universe as a whole.

In 1927, Lemaître astronomer suggested a big idea about the formation of the universe. According to his idea, the universe formation started as just a single point for a very long time ago. Before this theory, Humans have been thinking about the beginnings of life and the universe for thousands of years. Each culture has explained their own creation story that how did it come into being. So, the universe formation is being mentioned after a great explosion which is called Big Bang. At the time of beginning, the universe was just so hot and tiny particles mixed with light and energy. With the passage of times, everything expanding and took up more space then it cooled down gradually. After this, that tiny particles attached together and formed an atoms. Over lots of time, atoms grouped together and form a new objects like stars and galaxies.

In recent studies, we use different methods and models of the cosmology to understand about the current expansion and evolution of the universe. In this study, cosmologist select hypothesis about current universe and then observed it by using different models with a different way. In 1917, Einstein proposed general theory of relativity and after this theory of relativity the study of modern cosmology has been started. After that study, de Sitter and Schwarzschild have also explored the new ideas of modern cosmology which make interest for researcher to study the very large distance objects.

2.3.1 Cosmic Acceleration

Recently, the discovery of modern cosmology is being a huge interesting subject among the researcher and scientist for a long time. Einstein proposed that the universe is a static model. After this discovery, Friedmann suggested an idea that our universe is accelerating. Finally, two individual teams high-Z Supernova and Supernova cosmology project have been studied about the universe and its acceleration. Later, they were surprised to know that the universe is gradually expanding. After a lot of effort and hardworking it was one of the great success about universe. Finally, they are able to get a noble prize for their unexpected achievement. The current status about our universe has been obtained under the investigation of various observational data and these observations involve study of SNIa, CMB, large scale structure, Sloan Digital Sky Survey, the integrated Sachs Wolfe effect and gravitational lensing. Through their study, it came to know that our universe is accelerating at present time. The source which is responsible for the accelerating universe is known as DE. Despite of a prolonged discussion on a DE, still our knowledge is limited about it.

2.3.2 Dark Matter and Dark Energy

Although, in modern cosmology DM is known as central elements. Since, DM is one of the main two quantities of the universe which exists in the form of baryonic and non-baryonic matter. In the whole universe nearly 23% associated with non-baryonic DM and roundabout 4% of total energy content is to the normal baryonic matter. In 1930, Swiss-American astronomer Fritz Zwicky, most famous and broadly cited cosmologist in the field of DM. He discover that due to the existence of non-baryonic DM, the radial velocity of galaxies in the form of cluster is much larger than visible other stars. The "axions" are described as a basic particles of no-baryonic DM having energy $10^{-5}ev$. The DM is detected by the emission of photon because stars emit light in the form of IR and ultraviolet spectrum. Some cosmologist observed that non-baryonic DM doesn't detect directly from the universe because it doesn't absorb or emit or reflect light. In the universe, the galaxies exist in the form of cluster. For maintaining velocities of the galaxies and holding cluster together, it must take control greater amount the other form of DM, because visible candidates of galaxies like stars and gases don't possess enough gravitational force of attraction. We can detect DM by calculating orbital speed of the stars in galaxies.

It is observed that the universe expands with repulsive force and is not slowing down under normal gravity. This unknown force is called DE and is responsible for current cosmic acceleration. Dark energy is even more mysterious force of our universe. According to some cosmologist, from total energy of the universe, there are 73% contain with DE . We realized that DE can not detect and can not be tasted, But its effect can be seen very clearly. In general theory of relativity, Einstein described the existence of the universe and proposed a new cosmological constant to balance the gravitational forces. The first and simple candidate of DE is a cosmological constant which can construct a static model of the universe [97], [98]. Early in 1915 , Einstein derived a field equation which is written as

$$R_{ab} - \frac{1}{2}Rg_{ab} = \frac{8\pi G}{c^4}T_{ab}, \tag{2.3.1}$$

which tells the curvature of the space time to the amount of matter and energy moving through a region of space time. When it applied to entire universe, Einstein found a result that the universe could not be static and unchanging if had to be either stretching or contracting, he was surprised to know this. Then he went back to equation and added left hand side Λg_{ab} which turn to be as

$$R_{ab} - \frac{1}{2}Rg_{ab} = \frac{8\pi G}{c^4}T_{ab}, \tag{2.3.2}$$

where Λ (lambda) is a cosmological constant. Also he called it cosmological number. The observational data shows that with positive energy density and negative pressure, the cosmological constant accepted as vacuum energy.

2.4 Holographic Principle and Holographic Dark Energy

The holographic principle primitively interrogates that the composition of quantum mechanics and quantum gravity demands 3-dimensional world to be an image of data that can be stored on a 2-dimensional projection much like a holographic image [99]. According to this scenario, the total information about the occupied volume can be achieved from its surrounding surface that bound this volume. The idea of this principle comes from black hole (BH) physics, especially from Bekenstein's entropy relation which means that entropy of the BH is proportional with its horizon area. By proceeding work on this principle in succussive process conduct to a well known DE model which is known as HDE. Cohen et al. [100] proposed a relation between ultraviolet and IR cutoff which play a very important role for this process. In an effective field theory the entropy S scales massively in a box of size L with UV cutoff Λ, i.e., $S \sim L^3\Lambda^3$, while L^3 volume is a maximum entropy limit in a box behaves non massively growing with area of the box in the BH thermodynamics scenario is known as Bekenstein entropy bound. Anyway, for every Λ, there is a enough large scale volume for which the entropy of an effective field theory will pass the Bekenstein bound. If we bound the volume of the system, the Bekenstein entropy limit may be satisfied in an effective field theory, follows as

$$S = L^3\Lambda^3 \lesssim S_B H \equiv \pi L^2 M_p^2, \tag{2.4.1}$$

where $S_B H$ denotes the entropy of the BH with radius L. By this inequality, the prediction shows that UV cutoff linked directly with IR cutoff L

and cannot be chosen independently for IR cutoff (i.e., scales as Λ^{-3}). However, there happen a difficulty in combining the above inequality since the Schwarzschild radius is much larger than the box size which creates some problems of in- similarity with the effective field theory. For this purpose, Cohen et al. proposed a strong constraint on the IR cutoff which eliminate all states that remain within their Schwarzschild radius, i.e.

$$L^3\Lambda^4 = L^3_{\rho_D} \lesssim L^2 M_p^2. \tag{2.4.2}$$

Here, left side of the equality sign represents the total energy of the system and the right side indicate mass of the Schwarzschild BH. Also, IR cutoff L is being scaled as Λ^{-2} and this limit is much constrictive than (2.4.1). From the relation (2.4.2), it shows that the maximum entropy of the system will be $S_B^{\frac{3}{4}}H$. Li [66] proposed an inequality and found an interesting energy density for DE as given in (0.0.1) referred to HDE. Before this, different models of IR cutoffs for HDE have been put forward. In this thesis, we use generalized ghost PDE with the version of flat universe.

2.5 Tsallis Holographic Dark Energy

Entropy of the whole universe is an important factor of the cosmological application of holography which means that radius of the largest distance is directly proportional to its area also similar to a black hole. In 1902, Gibbs proposed that when systematic partition function diverges then Boltzmann-Gibbs theory can not be applied. Boltzmann-Gibbs additive entropy is generated from the hypothesis of weak probabilistic correlations and their connections with ergodicity. Also, the entropy of the whole system is not necessarily the sum of the entropies of its sub-systems known as non-additive entropy. However, this usual Boltzmann-Gibbs additive entropy must be generalized to this non-additive entropy which is know as Tsallis entropy [101]-[104]. Particularly, we realized from the proposal [105] this non extensive Tsallis entropy can be written in compact form which follows as

$$S_T = \lambda A^{\delta}. \tag{2.5.1}$$

Here, λ and δ in general case these parameters remain as completely free parameters while in the case of $\lambda = 2\pi M_p^2$ (M_p is a reduced Planck mass) and $\delta = 1$ we get the usual additive entropy. The gravitational and non extensive whole universe hypothesis which includes the holographic and entropy relations one should use the above generalized definition of the universe horizon entropy. From the combination of inequality $\rho_D L^4 \leq S$ with $S \propto A \propto L^2$ [106], the holographic dark energy is obtain easily. Hence, Tsallis HDE density is obtain by combining Eq.(2.5.2) with these inequalities which is given in following form

$$\rho_D = BL^{2\delta-4}, \tag{2.5.2}$$

where B is an arbitrary parameter. Although, in case of $\delta = 1$ (also mention above), the above expression produce usual holographic dark energy $\rho_D = 3c^2 M_p^2 L^{-2}$, with the parameter $B = 3c^2 M_p^2$ and arbitrary constant c^2. Moreover, it is most necessarily to mention that for special case $\delta = 2$, Tsallis HDE totaly converts in standard cosmological constant Λ.

2.6 Pilgrim Dark Energy

In 2012, Wei [107] proposed so-called "Pilgrim dark energy" model by using the idea of the HDE. He worked on the formation of BH and argued that the repulsive force granted by the phantom-like behavior of dark energy is strong sufficient to prevent the formation of the BH. By Cohen et al. [108], [109] if this supposition is true then energy limit could be violated (i.e., $\rho_D \gtrsim M_p^2 L^{-2}$). However, He proposed first property of pilgrim dark energy which as follows

$$\rho_D \gtrsim M_p^2 L^{-2}. \tag{2.6.1}$$

After some implement, the simplification form of this Eq.(2.6.1) is to set as

$$\rho_D = 3c^2 M_p^{4-\mu} L^{-\mu}. \tag{2.6.2}$$

Here, c and μ both represents as dimensionless constants. PDE model is used by choosing different L (IR cutoffs). Also, Wei [107] proposed the PDE model by using Hubble horizon as IR cutoff and explained the current acceleration of the universe. Hence, the energy density for the PDE model in term of Hubble horizon is turn as $\rho_D = 3c^2 M_p^{4-\mu} H^{\mu}$.

2.7 Generalized Ghost Pilgrim Dark Energy

In the development of modern cosmology, the synopsis of Veneziano ghost DE which is $\rho_D = \alpha H$, where α is a constant remains in the division of dynamical DE models plays a vital role in the present accelerated expansion of the universe [110]-[114]. This motivation is useful to solve U(1) problem in Veneziano ghost of choromodynamics (QCD) also comes from QCD. It is very important to note that the Veneziano ghost also produces non trivial physical effects in FRW universe. The QCD ghost contribution with the vacuum energy density is proportional to $\Lambda_{QCD}^3 H$ (where $\Lambda_{QCD} \sim 100MeV$ is the smallest QCD scale and H indicates as Hubble parameter) plays an important role in the evolutionary behavior of the universe. Various theoretical directions have been explored for this model and examined with different observational schemas [115]-[119]. It is prominent that vacuum energy from Veneziano ghost field in QCD is of the form $H + O(H^2)$ [120], but in the form of ordinary ghost DE model, only H (leading term) has been evaluated. Cai et al. [121] proposed that the contribution of H^2 (sub-leading term) in the ordinary ghost DE make easier to describing the past evolution of the universe. Therefore, he proposed the so-called "generalized ghost DE" density as

$$\rho_D = \alpha H + \beta H^2, \tag{2.7.1}$$

where β is another constant. Some cosmological consequences have been proposed for this model such as EoS, deceleration, O_m, $\omega - \omega'$, V_s^2 (stability analysis) and state-finder parameters [122]-[124]. Hence, recently [125], generalized form of ghost PDE has been suggested by using PDE phenomenon defined as follows

$$\rho_D = (\alpha H + \beta H^2)^{\mu}. \tag{2.7.2}$$

2.8 Cosmological Parameters

In 1970, Sandage once proposed cosmology as the exploration for two parameters such as H_0 and q_0, which were just beyond reach. In modern work, cosmological models are observing with number of different parameters. With the help of these parameters the quantity and quality of cosmological data measure. However, the observational results depend on the choice of parameters to describe acceleration as well as deceleration of the universe.

2.8.1 Hubble Parameter

In 1929, Hubble proposed a very useful relation for recessional velocity. By the time dependent value H, we can find the expansion of the universe is known as Hubble parameter which is defined as the relation between velocity and distance as

$$v = H_0(t)r, \tag{2.8.1}$$

where v and r denotes as velocity and distance while H_0 is an approximate calculation which is $H_0 = 72 \pm 8km/s/Mpc$. Also, Hubble parameter helps in describing the current expansion rate of the universe.

2.8.2 EoS Parameter

By the EoS parameter, we manipulate the energy density and pressure. It is defined as the ratio between energy pressure and energy density is called the EoS parameter which is denoted as ω. The mathematically form is given below

$$\omega = \frac{p}{\rho}, \tag{2.8.2}$$

here p and ρ appear as pressure and energy density of DE. The EoS parameter give a long and distinct period of history about the universe. If the result shows ω = 0,1/3 and 1, it predicts dust era/non-relativistic matter, ultra relativistic matter and stiff fluid respectively. If ω =-1/3, -1 and < -1, it corresponds the quintessence of DE, cosmological CDM and phantom period respectively.

2.8.3 Deceleration Parameter

The dimensionless deceleration parameter q, states that the rate of deceleration and acceleration of the cosmic expansion of the universe is valuate by taking the second time derivative of the scale factor $a(t)$ which is given in following form

$$q = -\frac{a\ddot{a}}{\dot{a}^2} = -\frac{\ddot{a}}{aH^2} = -1 - \frac{\dot{H}}{H^2}. \tag{2.8.3}$$

If $q \geq 0$, it predicts that the universe is decelerating, and when $q \in (-1, 0)$, it shows the acceleration phase of the universe.

2.8.4 $\omega - \omega'$ Analysis

Caldwell and Linder [126] suggested that the dynamical property of DE in quintessence region spell out with $\omega - \omega'$, here ω and ω' (prime denote $x = \ln a$) is the EoS parameter and its evolutionary form respectively. By $\omega - \omega'$ analysis, we discuss two distinct region thawing and freezing. For $\omega < 0$ and $\omega' > 0$, it predicts thawing region and if $\omega < 0,\ \omega' < 0$ then this represents freezing region. Initially, this result was applied for checking the behavior of quintessence framework.

2.8.5 State-finder parameter

For the purpose of deceleration and acceleration of the universe, Sahni et al. [127] proposed new cosmological dimensionless parameters. These are derived by taking the double time derivative of Hubble parameter and combining with deceleration parameter, we get

$$r = 1 + 3\frac{\dot{H}}{H^2} + \frac{\ddot{H}}{H^3}, \quad s = \frac{r-1}{3(q-\frac{1}{2})}. \tag{2.8.4}$$

These dimensionless parameters are useful for finding the distance of DE models with many different ΛCDM limit. For $(r, s) = (1, 0)$, this predicts ΛCDM region and $(r, s) = (1, 1)$, indicates the CDM era. If $s > 0$ and $r < 1$, it represents the phantom and quintessence of DE regions. Also, when $r > 1$ and $s < 0$, then it shows the Chaplygin gas.

2.8.6 Stability Analysis

In this scenario, we use squared speed sound to check the stability of the cosmos models. The ratio between energy pressure and energy densities is called squared sound speed which is $v_s^2 = \frac{dp}{d\rho} = \frac{\dot{p}}{\dot{\rho}}$, using EoS parameter, finally we get

$$v_s^2 = \omega + \frac{\dot{\omega}\rho}{\dot{\rho}} \tag{2.8.5}$$

For $v_s^2 \geq 0$, this predicts that the model is stable, if $v_s^2 < 0$, this represents that the given model show instability.

2.8.7 Om Parameter

The Om parameter is one of the another approach to describe the different phases of the universe. It is also used to differentiate ΛCDM from other models of the DE. Also, we can be used Om parameter to renowned ΛCDM for largest coupled scaler field, quintessence and phantom phase model through trajectories of curve which plotting in graph. Generally, Om is a combination of Hubble and cosmos redshift parameter to get a null test of the DE. The positive values of Om shows that the DE phase is like phantom and the negative lines means that DE corresponds to quintessence phase as well. The expression of Om with respect to redshift z is given bellow

$$Om(z) = \frac{(\frac{H(z)}{H_0})^2 - 1}{(1+z)^3 - 1}. \tag{2.8.6}$$

2.9 Cyclic Universe

Loop quantum cosmology (LQC) is an attractive and interesting application of loop quantum gravity in the framework of cosmology which originates the universe to bounce when it is small and to push around when it is in large scale. Also, LQC discuss the properties of two principles such as non-perturbative quantization and background independent quantization of gravity [86]-[91]. With the help of different DE models, LQC studied for knowing about quantum effects on our universe. Nowadays, LQC discussed the current acceleration of the universe phenomenon like big rip and big bang where future singularities can be ignored at classical epoch. Moreover, due to LQC the modification in standard FRW universe becomes more dominant and the universe begins to bounce and then oscillate forever. In LQC, some author explored cosmic coincidence problem of modern cosmology with the help of modified Chaplygin gas connected to DM [92]. However, At high epoch of energy densities, we hire the modified Friedmann equation [82]-[85]. The equation of motion in LQC is given below

$$H^2 = \frac{\rho}{3M_p^2}\left(1 - \frac{\rho}{\rho_c}\right), \tag{2.9.1}$$

here,

$$\rho_c = \frac{\sqrt{3}}{16\pi^2\gamma^3 G^2 h}, \tag{2.9.2}$$

represents the critical density strained by quantum gravity (γ denotes as dimensionless Barbero-Immirzi parameter) and the total energy density is $\rho = \rho_m + \rho_D$ where subscripts m and D denotes for DM and DE, respectively.

2.10 DGP Braneworld

By some observations, we are able to know that our universe is a brane embedded with higher dimensional bulk. DGP braneworld scenario helps to leak the gravity from lower dimension to higher dimension is a main source of accelerated expansion. There are two main branches analyzed in DGP braneworld scenario which is $\epsilon = \pm 1$ [27], [28]. In self-accelerated ($\epsilon = +1$) branch, DE phenomena is no longer needed for accelerating phase of the universe [27]. Normal branch ($\epsilon = -1$) explored for HDE scenario, where it predicted that the universe is in accelerating phase with the only responsibility of DE [29]. In this thesis we also extend our work with braneworld synopsis for flat FRW universe installed in a Minkowski bulk, the Friedmann equation modified [93, 94] in the form as

$$H^2 = \left(\sqrt{\frac{\rho}{3M_p^2} + \frac{1}{4r_c^2}} + \frac{\epsilon}{2r_c} \right)^2, \tag{2.10.1}$$

where $\epsilon = \pm$ leads for two branches and $r_c = \frac{M_p^2}{2M_5^3} = \frac{G_5}{2G_4}$ is a ratio between small and large distances. It is necessary to mention that this equation can be reduced to

$$H^2 = \frac{\rho}{M_p^2}. \tag{2.10.2}$$

By recent observational data, we claim above that our universe is represent in flat form and hence Eq.(2.10.1) can be reduced in standard Friedmann equation

$$H^2 = \frac{\rho}{3M_p^2} + \frac{\epsilon H}{r_c}. \tag{2.10.3}$$

In this DGP model, we only discuss normal branch ($\epsilon = -1$) for the flat universe. The regular gravitational laws in this layout can be got by the addition of the work with the Einstein-Hilbert action term evaluate with the brane immanent curvature. Existence of this particular term and the activity is induced because of quantum corrections appearing from the bulk gravity and its linking with matter living on the brane framework.

2.11 RS II Braneworld

RS II braneworld model is a cosmological model which entails a modified high energy era in the past radiation dominant phase of the universe. The current observations states that the Newton law only implies for four dimensional bulk. But, RS II branworld model [30] proposed that this is not necessarily true in the presence of a non factorizable background geometry. They studied the specific term which is a single 3-brane embedded in five dimensions. Also, this idea shows that even without a gap in the Kaluza-Klein spectrum, four-dimensional Newtonian and general relativistic gravity is reproduced to more than acceptable precision. The correspondence braneworld relation [30] for this RS II model is given by

$$S = \int d^5x\sqrt{-g}(M_5^3 R - \rho_{D5}) + \int d^4x\sqrt{-\gamma}(L_{br} - V + r_c M_5^3 R_4). \tag{2.11.1}$$

Here, R is represents as five dimensional bulk space time curvature scalar, M_5 is a fifth dimensional Planck mass and ρ_{D5} denotes as a bulk energy density. Also, here g is a five dimensional space time metric determinant while four dimensional space time metric is λ. L_{br} denotes as brane matter content and here the term V is called the brane tension. Also r_c represents as a characteristic length scale while R_4 is the four dimensional curvature scalar. The evolutionary form of brane RS II is modified field equation written as

$$H^2 = \frac{8\pi}{3M_p^2}\rho + \frac{8\pi}{3M_p^2}\rho_D, \tag{2.11.2}$$

here $M_p^2 = \frac{1}{8\pi G}$ appears as a reduced Planck mass. The four dimensional effective energy density is followed by

$$\rho_D = \rho_{D4} = \frac{M_p^2}{32\pi M_5^3}\rho_{D5} + \frac{3M_p^3}{2\pi(\frac{L_5}{8\pi} - 2r_c)^2}, \tag{2.11.3}$$

where ρ_{D5} is represents for the five dimensional bulk HDE. For HDE, it takes place in the following form

$$\rho_{D5} = \frac{3c^2B}{4\pi}M_5^3 L^{-2}. \tag{2.11.4}$$

For the purpose of four dimensional HDE, combining this phenomenon with Eq.(2.11.3), we get

$$\rho_D = \frac{3c^2BM_p^2}{128\pi^2 M_5^3}L^{2\delta-4} + \frac{3M_p^3}{2\pi(\frac{L_5}{8\pi} - 2r_c)^2}. \tag{2.11.5}$$

2.12 Dynamical Chern-Simons Modified Gravity

Einstein Hilbert action is a numerically corrected form of low-energy limit of string theory which defines an effective CS modified gravity. The corrected CS gravity contains the product of Pontryagin density with scalar field, where it can be treated as an evolving field or a background field.

Here, evolving field means dynamical and background field mean non dynamical field. In this work, we only describe a motivation about dynamical CS modified gravity. The relation which give the dynamical CS modified gravity is define bellow

$$S=\frac{1}{16\pi G}\int_d d^4x\left[\sqrt{-g}R+\frac{l}{4}\theta^{*}R^{abcd}R_{abcd}-\frac{1}{2}g^{cd}\nabla_c\theta\nabla_d\theta+V(\theta)\right]+S_{mat}, \tag{2.12.1}$$

where R denotes the Ricci scalar, ${}^{*}R^{abcd}R_{abcd}$ is a topological invariant called the Pontryagin term, l for a coupling constant, θ represents the dynamical variable, S_{mat} shows the action of matter and $V(\theta)$ for the potential term. In the instance of string theory, we apply $V(\theta)=0$. By expanding the action equation with respect to g_{cd} and the scalar field θ, it turn to the following field equations

$$\begin{aligned} G_{cd}+lC_{cd} &= 8\pi G T_{cd}, \\ g^{cd}\nabla_c\nabla_d\theta &= -\frac{l}{64\pi}{}^{*}R^{abcd}R_{abcd}. \end{aligned} \tag{2.12.2}$$

Here, G_{cd} and C_{cd} represents for Einstein tensor and Cotton tensor, respectively. The Cotton tensor C_{cd} can be described as

$$C_{cd}=-\frac{1}{2\sqrt{-g}}((\nabla_a\theta)\varepsilon^{a\beta\tau(c}\nabla_\tau R^{d)}_{\beta})+(\nabla_b\nabla_a\theta)^{*}R^{a(cd)b}. \tag{2.12.3}$$

The energy-momentum tensor is

$$\begin{aligned} \hat{T}^{\theta}_{cd} &= \nabla_c\theta\nabla_d\theta-\frac{1}{2}g_{cd}\nabla^a\theta\nabla_a\theta, \\ T_{cd} &= (\rho+p)u_c u_d+p g_{cd}, \end{aligned} \tag{2.12.4}$$

where, T_{cd} denotes for matter contribution and $\hat{T}^{\theta}_{cd}$ shows the scalar field contribution while, p and ρ describes for pressure density and energy density. Moreover, $u_c=(1,0,0,0)$ represents the four velocity. In the theory of CS gravity, Friedmann equation modified in the following form

$$H^2 = \frac{1}{3}(\rho_m + \rho_D) + \frac{1}{6}\dot{\theta}^2, \tag{2.12.5}$$

where dot (.) predicts the derivative with respect to t and $8\pi G = 1$. For FRW universe, the ponytrying term ${}^*RR$ go away identically here, the scalar field in (2.12.2) turn into the following form

$$g^{cd}\nabla_c\nabla_d\theta = g^{cd}[\partial_d\partial_c\theta] = 0. \tag{2.12.6}$$

We define $\theta = \theta(t)$ and obtain the following relation

$$\ddot{\theta} + 3H\dot{\theta} = 0, \tag{2.12.7}$$

which shows that $\dot{\theta} = ba^{-3}$, b represents as a constant of integration. By using this relation in Eq.(2.12.5), we get

$$H^2 = \frac{1}{3}(\rho_m + \rho_D) + \frac{1}{6}b^2a^{-6}. \tag{2.12.8}$$

Chapter 3
Tsallis Holographic Dark Energy in Cyclic Universe Model

In this chapter, we use Tsallis holographic dark energy model with generalized ghost pilgrim dark energy as infra-red cutoff for the cyclic universe in the flat Friedmann-Robertson-Walker universe. In this direction, we study some cosmological parameters like equation of state, deceleration parameter, squared sound speed and Om parameter. We also establish some cosmic planes such as $\omega - \omega'$ and $r - s$ on the basis of presents day observational data.

3.1 Cyclic Universe Case

We know that an attractive and interesting application of loop quantum gravity in the framework of cosmology is a LQC which has the Friedmann equation modified in LQC is in Eq.(2.9.1). In our work, we claims that the DE do not mutual interact with DM. Hence, the conservation equations are obtained as

$$\dot{\rho}_D + 3H(1+\omega)\rho_D = 0, \tag{3.1.1}$$

$$\dot{\rho}_m + 3H\rho_m = 0 \rightarrow \rho_m = \rho_0(1+z)^3. \tag{3.1.2}$$

We define the dimensionless density parameters

$$\Omega_D = \frac{\rho_D}{\rho_{cr}}, \quad \Omega_m = \frac{\rho_m}{\rho_{cr}}. \tag{3.1.3}$$

For the observational data, here $\rho_{cr} = 3M_p^2H^2$ is the regular critical density. By proceeding our work, combining Eq.(3.1.3) with (1.0.3), we find out the DE dimensionless density parameter which is

$$\Omega_D = \frac{B(\alpha H + \beta H^2)^{4-2\delta}}{3M_p^2H^2}. \tag{3.1.4}$$

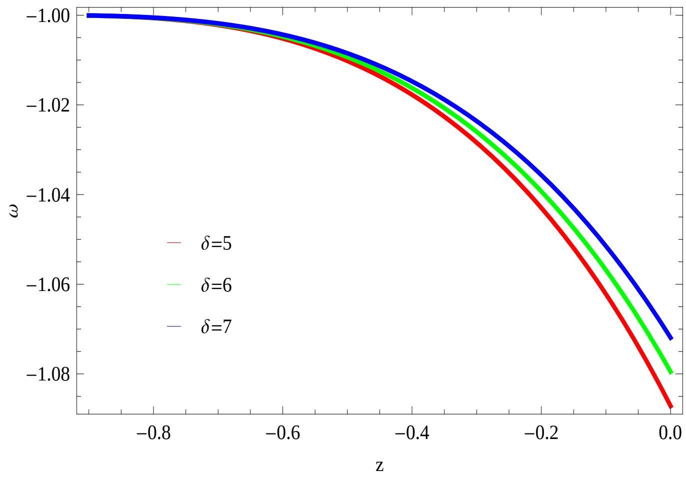

Figure 3.1: Plots of EoS parameters versus z for generalized ghost PDE in cyclic universe.

Taking the time derivative of Eq.(2.9.1), then combining the results with (3.1.3), we are able to find the Hubble parameter as follows

$$\frac{\dot{H}}{H^2} = \frac{-3u(2-\Omega_D(1+u))(\alpha+\beta H)}{2(1+u)(\alpha+\beta H)+2(\delta-2)(\alpha+2\beta H)(2-\Omega_D(1+u)}, \quad (3.1.5)$$

here, u appears as a frictional form of energy densities which is $\frac{\rho_m}{\rho_D}$. Bearing in mind the fact $\dot{\Omega}_D = \Omega'_D H$, where dot and prime denotes for the derivative with respect to time and $x = \ln a$ respectively. Finally taking the time derivative of Eq.(3.1.4), and then using (3.1.5), we get the following result

$$\Omega'_D = \frac{-3u\Omega_D(2-\Omega_D(1+u))((2-\delta)(\alpha+2\beta H)-(\alpha+\beta H)}{(1+u)(\alpha+\beta H)+(\delta-2)(\alpha+2\beta H)(2-\Omega_D(1+u)}. \quad (3.1.6)$$

For the calculation of well-known EoS parameter, taking the time derivative of Eq.(1.0.3) and combining with (3.1.1), we have the following equation

$$\omega = -1 + \frac{u(2-\delta)(2-\Omega_D(1+u))(\alpha+2\beta H)}{2(1+u)(\alpha+\beta H)+(\delta-2)(\alpha+2\beta H)(2-\Omega_D(1+u))}. (3.1.7)$$

Let us we find the effect of parameter δ on $\omega(z)$. In Figure 3.1, we check the behavior of EoS parameter as a function of redshift z for three different values of δ including the values $\delta = 5, 6, 7$. Here we observe that, for

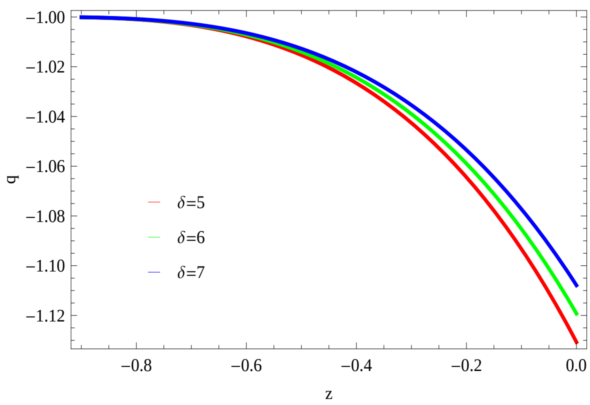

Figure 3.2: Plots of deceleration parameters versus z for generalized ghost PDE in the cyclic universe.

increasing value of z the evolution $\omega(z)$ tend to increasing values. At the present time where $\omega(z) = 0$, it remains in phantom period. Hence, It can be observed that for Tsallis HDE in the cyclic universe the evolutionary ω starts from ΛCDM regime and moved in phantom region. Deceleration parameter is calculated by inserting Eq.(3.1.5) in (2.8.3),we get following result as follows

$$q = -1 + \frac{3u(2-\Omega_D(1+u))(\alpha+\beta H)}{2(1+u)(\alpha+\beta H)+2(\delta-2)(\alpha+2\beta H)(2-\Omega_D(1+u)}. \quad (3.1.8)$$

The plot of deceleration parameter against the red shift parameter z is obtain in Figure 3.2. We observe that for increases of redshift z the deceleration parameter is increasing and increases to lesser negative values. Thus, it can be seen that the transition of the universe shows in accelerating phase. For the $\omega - \omega'$ analysis, we take the derivative of Eq.(3.1.7) with respect to $x = \ln a$, we propose the evolutionary form of ω which is given as

$$\begin{aligned} \omega' &= \frac{1}{H}((2\beta(2-\delta)\rho_m(2-(1+u)\Omega_D)\dot{H})/(\rho_D((\alpha+\beta H)(1+u)+(\delta-2) \\ &\times (\alpha+2\beta H)(2-(1+u)\Omega_D))) - ((2-\delta)(\alpha+2\beta H)\rho_D(2-(1+u)\Omega_D \end{aligned}$$

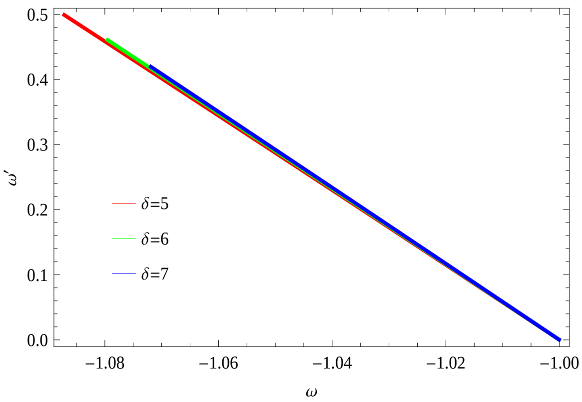

Figure 3.3: Plots of ω' versus ω for generalized ghost PDE in the cyclic universe.

$$\begin{aligned}
\times &\quad)\dot{\rho}_D/(\rho_D^2((\alpha+\beta H)(1+u)+(\delta-2)(\alpha+2\beta H)(2-(1+u)\Omega_D))) \\
+ &\quad ((2-\delta)(\alpha+2\beta H)(2-(1+u)\Omega_D)\dot{\rho}_D)/(\rho_D((\alpha+\beta H)(1+u)+(\delta \\
- &\quad 2)(\alpha+2\beta H)(2-(1+u)\Omega_D)))+((-\delta)(\alpha+2\beta H)\rho_D(-\Omega_D(-u\dot{\rho}_D \\
/ &\quad \rho_D+\dot{\rho}_m/\rho_D)-(1+u)\dot{\Omega}_D))/(\rho_D((\alpha+\beta H)(1+u)+(\delta-2)(\alpha+2 \\
\times &\quad \beta H)(2-(1+u)\Omega_D)))-((2-\delta)(\alpha+2\beta H)\rho_m(2-(1+u)\Omega_D)(\beta(1 \\
+ &\quad u)\dot{H}+2\beta(\delta-2)(2-(1+u)\Omega_D)\dot{H}+(\alpha+2\beta H)(-u\dot{\rho}_D/\rho_D+\dot{\rho}_m/\rho_D) \\
+ &\quad (\delta-2)(\alpha+2\beta H)(-\Omega_D(-u\dot{\rho}_D\rho_D+\dot{\rho}_m/\rho_D)-(1+u)\dot{\Omega}_D)))/(\rho_D((\alpha \\
+ &\quad \beta H)(1+u)+(\delta-2)(\alpha+2\beta H)(2-(1+u)\Omega_D))^2))).
\end{aligned} \tag{3.1.9}$$

The plot of ω' versus ω in our observational model is given in Figure 3.3 for different values of δ. Here, it can be observed that the values of ω' is increases as increase the value of ω. Also it can be shown that the $\omega' > 0$ and $\omega < 0$ which indicates the thawing region of the universe. In cyclic universe, the expressions of r and s is calculate from Eq.(2.8.4), where we obtain

$$r = 1-(9(\alpha+\beta H)\rho_m(2-(1+u)\Omega_D))/(\rho_D(2(\alpha+\beta H)(1+u)+2(-2$$

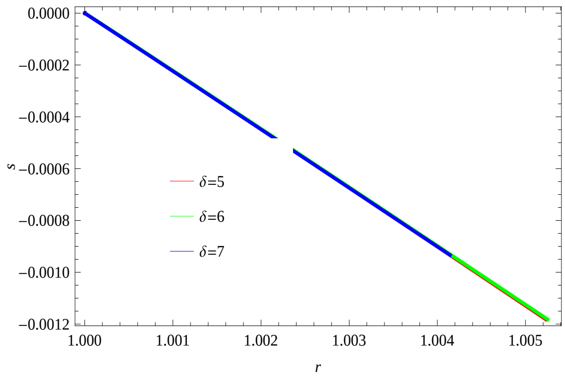

Figure 3.4: Plots of state-finder parameters s versus r for generalized ghost PDE in the cyclic universe.

$$
\begin{aligned}
+ &\quad \delta)(\alpha+2\beta H)(2-(1+u)\Omega_D))) + 1/H(-(3\beta\rho_m(2-(1+u)\Omega_D)\dot{H})/ \\
\times &\quad (\rho_D(2(\alpha+\beta H)(1+u)+2(-2+\delta)(\alpha+2\beta H)(2-(1+u)\Omega_D))) + 2 \\
\times &\quad \dot{H}^2/H^3 + (3(\alpha+\beta H)\rho_m(2-(1+u)\Omega_D)\dot{\rho}_D)/(\rho_D^2(2(\alpha+\beta H)(1+u) \\
+ &\quad 2(-2+\delta)(\alpha+2\beta H)(2-(1+u)\Omega_D))) - (3(\alpha+\beta H)(2-(1+u)\Omega_D) \\
\times &\quad \dot{\rho}_m)/(\rho_D(2(\alpha+\beta H)(1+u)+2(-2+\delta)(\alpha+2\beta H)(2-(1+u)\Omega_D))) \\
+ &\quad (6(\alpha+\beta H)\rho_m(2-(1+u)\Omega_D)(\beta\rho_D((-7+4\delta)\rho_D+\rho_m-2(-2+\delta) \\
\times &\quad (\rho_D+\rho_m)\Omega_D)\dot{H} + (-\alpha-\beta H+(-2+\delta)(\alpha+2\beta H)\Omega_D)(\rho_m\dot{\rho}_D-\rho_D \\
\times &\quad \dot{\rho}_m) - (-2+\delta)(\alpha+2\beta H)\rho_D(\rho_D+\rho_m)\dot{\Omega}_D))/(\rho_D^3(2(\alpha+\beta H)(1+u) \\
+ &\quad 2(-2+\delta)(\alpha+2\beta H)(2-(1+u)\Omega_D))^2) - (3(\alpha+\beta H)\rho_m((\Omega_D(\rho_m\dot{\rho}_D \\
- &\quad \rho_D\dot{\rho}_m))/(\rho_D^2) - (1+u)\dot{\Omega}_D))/(\rho_D(2(\alpha+\beta H)(1+u)+2(-2+\delta)(\alpha \\
+ &\quad 2\beta H)(2-(1+u)\Omega_D)))), \qquad (3.1.10)
\end{aligned}
$$

and

$$
\begin{aligned}
s &= (-9(\alpha+\beta H)\rho_m(2-(1+u)\Omega_D)/(\rho_D(2(\alpha+\beta H)(1+u)+2(-2 \\
&+ \delta)(\alpha+2\beta H)(2-(1+u)\Omega_D))) + 1/H((-3\beta\rho_m(2-(1+u)\Omega_D) \\
&\times \dot{H})/(\rho_D(2(\alpha+\beta H)(1+u)+2(-2+\delta)(\alpha+2\beta H)(2-(1+u)\Omega_D)))
\end{aligned}
$$

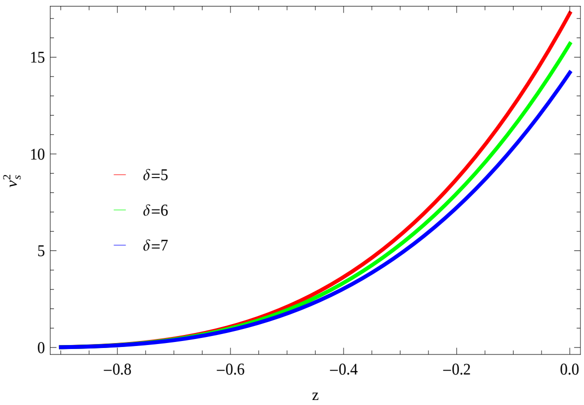

Figure 3.5: Plot of v_s^2 versus z for generalized ghost PDE in the cyclic universe.

$$
\begin{aligned}
+ \quad & 2\dot{H}^2/H^3 + (3(\alpha+\beta H)\rho_m(2-(1+u)\Omega_D)\dot{\rho}_D)/(\rho_D^2(2(\alpha+\beta H)(1+u) \\
+ \quad & 2(-2+\delta)(\alpha+2\beta H)(2-(1+u)\Omega_D))) - (3(\alpha+\beta H)(2-(1+u)\Omega_D) \\
\times \quad & \dot{\rho}_m)/(\rho_D(2(\alpha+\beta H)(1+u)+2(-2+\delta)(\alpha+2\beta H)(2-(1+u)\Omega_D))) \\
+ \quad & (6(\alpha+\beta H)\rho_m(2-(1+u)\Omega_D)(\beta\rho_D((-7+4\delta)\rho_D+\rho_m-2(-2+\delta) \\
\times \quad & (\rho_D+\rho_m)\Omega_D)\dot{H} + (-\alpha-\beta H+(-2+\delta)(\alpha+2\beta H)\Omega_D)(\rho_m\dot{\rho}_D-\rho_D \\
\times \quad & \dot{\rho}_m) - (-2+\delta)(\alpha+2\beta H)\rho_D(\rho_D+\rho_m)\dot{\Omega}_D))/({\rho_D}^3(2(\alpha+\beta H)(1+u) \\
+ \quad & 2(-2+\delta)(\alpha+2\beta H)(2-(1+u)\Omega_D))^2) - (3(\alpha+\beta H)\rho_m((\Omega_D(\rho_m\dot{\rho}_D \\
- \quad & \rho_D\dot{\rho}_m))/(\rho_D^2) - (1+u)\dot{\Omega}_D)/(\rho_D(2(\alpha+\beta H(1+u)+2(-2+\delta)(\alpha+2 \\
\times \quad & \beta H)(2-(1+u)\Omega_D)))))/(3(-1.5+(3(\alpha+\beta H)\rho_m(2-(1+u)\Omega_D))/(\rho_D \\
\times \quad & (2(\alpha+\beta H)(1+u)+2(-2+\delta)(\alpha+2\beta H)(2-(1+u)\Omega_D))))). \qquad (3.1.11)
\end{aligned}
$$

In Figure 3.4, we plot r versus s planes for generalized ghost PDE in this scenario by taking different values of $\delta = 5, 6, 7$. It can be observed that the graph shows chaplygin gas because here $r > 1$ and $s < 0$. Also we obtain explicit form of squared sound of speed (v_s^2) by taking the time derivative of Eq.(3.1.7) and by combing the result with Eqs.(1.0.3) and (2.8.5) which is given bellow

$$
\begin{aligned}
v_s^2 &= -1+((2-\delta)(\alpha+2\beta H)\rho_m(2-(1+u)\Omega_D))/(\rho_D((\alpha+\beta H)(1+u) \\
&+ (-2+\delta)(\alpha+2\beta H)(2-(1+u)\Omega_D)))+1/\dot{\rho}_D\rho_D((2\beta(2-\delta)\rho_m(2 \\
&- (1+u)\Omega_D)\dot{H})/(\rho_D((\alpha+\beta H)(1+u)+(-2+\delta)(\alpha+2\beta H)(2-(1 \\
&+ u)\Omega_D)))-((2-\delta)(\alpha+2\beta H)\rho_m(2-(1+u)\Omega_D)\dot{\rho}_D)/(\rho_D^2((\alpha+\beta H) \\
&\times (1+u)+(-2+\delta)(\alpha+2\beta H)(2-(1+u)\Omega_D)))+((2-\delta)(\alpha+2\beta \\
&\times H)(2-(1+u)\Omega_D)\dot{\rho}_m)/(\rho_D((\alpha+\beta H)(1+u)+(-2+\delta)(\alpha+2\beta \\
&\times H)(2-(1+u)\Omega_D)))+((2-\delta)(\alpha+2\beta H)\rho_m(-\Omega_D(-u\dot{\rho}_D/\rho_D+\dot{\rho}_m \\
&/ \rho_D)-(1+u)\dot{\Omega}_D))/(\rho_D((\alpha+\beta H)(1+u)+(-2+\delta)(\alpha+2\beta H)(2 \\
&- (1+u)\Omega_D)))-((2-\delta)(\alpha+2\beta H)\rho_m(2-(1+u)\Omega_D)(\beta(1+u)\dot{H} \\
&+ 2\beta(-2+\delta)(2-(1+u)\Omega_D)\dot{H}+(\alpha+\beta H)(-u\dot{\rho}_D/\rho_D+\dot{\rho}_m/\rho_D)+(\\
&- 2+\delta)(\alpha+2\beta H)(-\Omega_D(-u\dot{\rho}_D/\rho_D+\dot{\rho}_m/\rho_D)-(1+u)\dot{\Omega}_D)))/(\rho_D((\alpha \\
&+ \beta H)(1+u)+(-2+\delta)(\alpha+2\beta H)(2-(1+u)\Omega_D))^2)).
\end{aligned}
\tag{3.1.12}
$$

Figure 3.5 shows the graph between squared sound speed v_s^2 and z. In the cyclic universe for Tsallis HDE model, it can be used to show the stability under different parametric values of δ. According to δ, at latter and present epoch, one can see that the graph shows $v_s^2 > 0$. Hence, the behavior of this model is a stable. The plot of Eq.(2.8.6) with Hubble parameter describes that the Om trajectories covers the negative values which corresponds to quintessence behavior of the universe. It is shown in Figure 3.6.

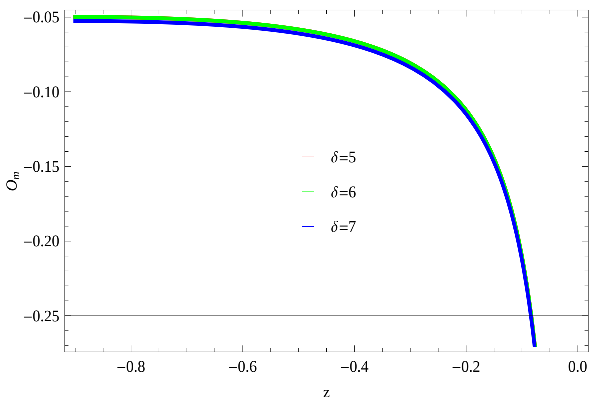

Figure 3.6: Plot of O_m versus z for generalized ghost PDE in the cyclic universe.

Chapter 4
Tsallis Holographic Dark Energy in DGP and RS II Braneworld Models

In this chapter, we use Tsallis holographic dark energy model with generalized ghost pilgrim dark energy as infra-red cutoff for modified theories of gravity such as Dvali-Gabadadze-Porrati braneworld and Randal-Sundrum II braneworld in the flat Friedmann-Robertson-Walker universe. In these directions, we study some cosmological parameters like equation of state, deceleration parameter, squared sound speed and Om parameter. We also establish some cosmic planes such as $\omega-\omega'$ and $r-s$ on the basis of presents day observational data.

4.1 DGP Braneworld Case

In the direction of modified theory, we extend our work with DGP braneworld for flat FRW universe, where the reduced form of standard Friedmann equation is written in Eq.(2.10.3). In this DGP braneworld model, we only investigate normal branch ($\epsilon = -1$) for the flat universe as we mention above. Using Eq.(3.1.3) and $\Omega_{rc} = \frac{1}{4H^2 r_c^2}$, the Eq.(2.10.3) can be written in the form

$$\Omega_D + \Omega_m + 2\epsilon\sqrt{\Omega_{rc}} = 1. \tag{4.1.1}$$

Using Eq.(1.0.3) and(3.1.3), this result becomes

$$\Omega_D = \frac{B(\alpha H + \beta H^2)^{4-2\delta}}{3M_p^2 H^2}. \tag{4.1.2}$$

For taking the time derivative of Eq.(2.10.3), then using the result of Eq.(1.0.3) and (3.1.2), we obtain Hubble parameter

$$\frac{\dot{H}}{H^2} = \frac{-3(1-\Omega_D - 2\epsilon\sqrt{\Omega_{rc}})(\alpha+\beta H)}{2(\alpha+\beta H) + 2(\delta-2)(\alpha+2\beta H)\Omega_D - 2\epsilon\sqrt{\Omega_{rc}}(\alpha+\beta H)}. \tag{4.1.3}$$

The evolution of the DE can be obtained by taking the time derivative of Eq.(4.1.2), and then combining with Eq.(3.1.3) and Eq.(4.1.3), it turn to

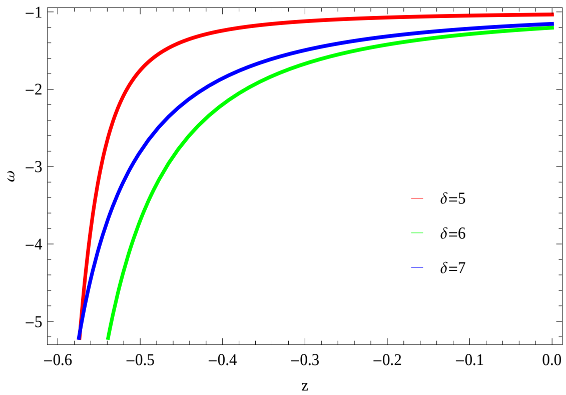

Figure 4.1: Plots of EoS parameters versus z for generalized ghost PDE in DGP framework .

be as follows

$$\Omega_D' = \frac{-3\Omega_D(1-\Omega_D-2\epsilon\sqrt{\Omega_{rc}})((2-\delta)(\alpha+2\beta H)-(\alpha+\beta H))}{(\alpha+\beta H)+(\delta-2)(\alpha+2\beta H)\Omega_D-\epsilon\sqrt{\Omega_{rc}}(\alpha+\beta H)}. \quad (4.1.4)$$

The EoS parameter is obtain by solving numerically Eqs.(1.0.3), (3.1.1) and (4.1.3), we get as

$$\omega = -1+\frac{(2-\delta)(1-\Omega_D-\epsilon\sqrt{\Omega_{rc}})(\alpha+2\beta H)}{(\alpha+\beta H)+(\delta-2)(\alpha+2\beta H)\Omega_D-\epsilon\sqrt{\Omega_{rc}}(\alpha+\beta H)}. \quad (4.1.5)$$

Now we plot the figure of EoS versus z in Figure 4.1. Here, we see that $\omega(z)$ is closer to ΛCDM behavior of the universe and then always remains in phantom era. The deceleration parameter is lead to following result, which is

$$q = -1+\frac{3(1-\Omega_D-2\epsilon\sqrt{\Omega_{rc}})(\alpha+\beta H)}{2(\alpha+\beta H)+2(\delta-2)(\alpha+2\beta H)\Omega_D-2\epsilon\sqrt{\Omega_{rc}}(\alpha+\beta H)}. (4.1.6)$$

From Figure 4.2, one can easily see that it is obviously that the model in DGP braneworld scenario can cover the accelerating phase of the universe. The expression ω' for Tsallis HDE in DGP framework obtain by taking the derivative of EoS parameter with respect to $\ln a$

$$\omega' = (-2+\delta)(-4\alpha\beta\epsilon^2\Omega_{rc}^{3/2}\dot{H}+2\sqrt{\Omega_{rc}}\alpha\beta(-1+\Omega_D)\dot{H}+(\alpha+2\beta H)$$

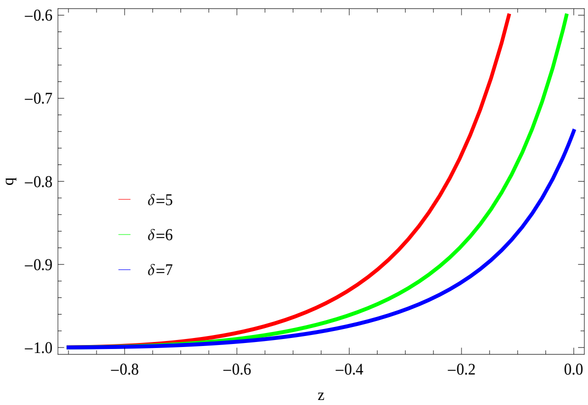

Figure 4.2: Plots of deceleration parameters versus z for generalized ghost PDE in DGP framework.

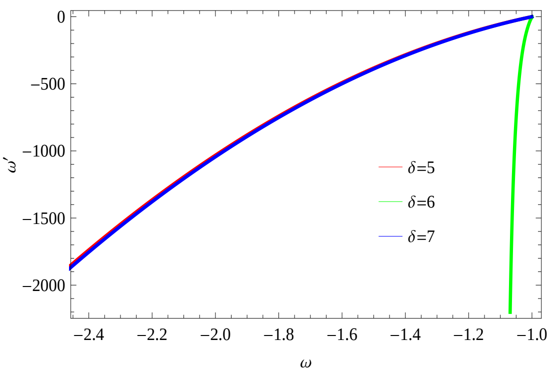

Figure 4.3: Plots of ω' versus ω for generalized ghost PDE in DGP framework.

$$\begin{aligned}
&\times \quad (\alpha(-1+\delta)+\beta(-3+2\delta)H)(\dot{\Omega}_D)-2\epsilon\Omega_{r_c}\alpha\beta(-3+\Omega_D)\dot{H} \\
&+ \quad (\alpha+2\beta H)(\alpha(-3+2\delta)+\beta(-7+4\delta)H)(\dot{\Omega}_D)+\epsilon(\alpha+2\beta H) \\
&\times \quad (\alpha+\beta H+(\alpha(-3+2\delta)+\beta(-7+4\delta)H)\Omega_D)(\dot{\Omega}_{r_c}))/(2H(\alpha(1 \\
&+ \quad (-2+\delta)\Omega_D-\epsilon\sqrt{\Omega_{r_c}})+\beta H(1+2(-2+\delta)\Omega_D \\
&- \quad \epsilon\sqrt{\Omega_{r_c}}))^2\sqrt{\Omega_{r_c}}). \qquad (4.1.7)
\end{aligned}$$

The graphs of ω versus ω' is shown in Figure 4.3, which trajectories cover the freezing region of the universe. Here the slope corresponds that the $\omega' < 0$ and $\omega < 0$ also. Using Eqs.(2.8.4), (4.1.3) and (4.1.6), we obtain the

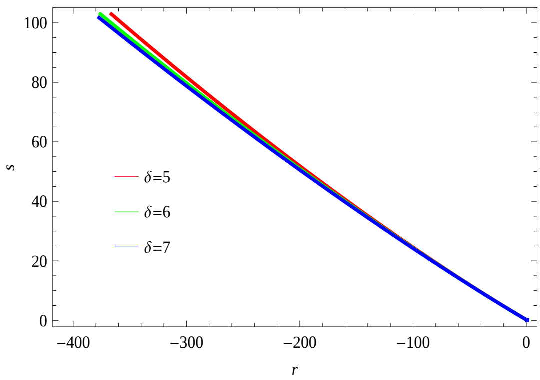

Figure 4.4: Plots of state-finder parameters s versus r for generalized ghost PDE in DGP framework.

state-finder expressions which are given as

$$
\begin{aligned}
r &= 1-9(1-\Omega_D-2\epsilon\sqrt{\Omega_{r_c}})(\alpha+\beta H)/(2(\delta-2)(\alpha+2\beta H)\Omega_D-2\epsilon\sqrt{\Omega_{r_c}}\\
&\times (\alpha+\beta H)+2(\alpha+\beta H))+1/H(2\dot{H}^2/H^3-3\beta(1-\Omega_D-2\epsilon\sqrt{\Omega_{r_c}})\dot{H}\\
&\times (2(\alpha+\beta H)+2(-2+\delta)(\alpha+2\beta H)\Omega_D-2\epsilon(\alpha+\beta H)\sqrt{\Omega_{r_c}})-(3(\alpha\\
&+ \beta)(-\dot{\Omega}_D-\epsilon\dot{\Omega}_{r_c}/\sqrt{\Omega_{r_c}}))/(2(\alpha+\beta H)+2(-2+\delta)(\alpha+2\beta H)\Omega_D\\
&- 2\epsilon(\alpha+\beta H)\sqrt{\Omega_{r_c}})+(3(\alpha+\beta H)(1-\Omega_D-2\epsilon\sqrt{\Omega_{r_c}})(2\beta\dot{H}+4\beta(-2\\
&+ \delta)\Omega_D\dot{H}-2\beta\epsilon\sqrt{\Omega_{r_c}}\dot{H}+2(-2+\delta)(\alpha+2\beta H)\dot{\Omega}_D-\epsilon(\alpha+\beta H)\dot{\Omega}_{r_c}\\
&/ \sqrt{\Omega_{r_c}}))/(2(\alpha+\beta H)+2(-2+\delta)(\alpha+2\beta H)\Omega_D\\
&- 2\epsilon(\alpha+\beta H)\sqrt{\Omega_{r_c}})^2),
\end{aligned} \tag{4.1.8}
$$

and

$$
\begin{aligned}
s &= (-9(1-\Omega_D-2\epsilon\sqrt{\Omega_{r_c}})(\alpha+\beta H)/(2(\delta-2)(\alpha+2\beta H)\Omega_D-2\epsilon\sqrt{\Omega_{r_c}}\\
&\times (\alpha+\beta H)+2(\alpha+\beta H))+1/H(2\dot{H}^2/H^3-3\beta(1-\Omega_D-2\epsilon\sqrt{\Omega_{r_c}})\dot{H}\\
&\times (2(\alpha+\beta H)+2(-2+\delta)(\alpha+2\beta H)\Omega_D-2\epsilon(\alpha+\beta H)\sqrt{\Omega_{r_c}})-(3(\alpha\\
&+ \beta)(-\dot{\Omega}_D-\epsilon\dot{\Omega}_{r_c}/\sqrt{\Omega_{r_c}}))/(2(\alpha+\beta H)+2(-2+\delta)(\alpha+2\beta H)\Omega_D\\
&- 2\epsilon(\alpha+\beta H)\sqrt{\Omega_{r_c}})+(3(\alpha+\beta H)(1-\Omega_D-2\epsilon\sqrt{\Omega_{r_c}})(2\beta\dot{H}+4\beta(-2
\end{aligned}
$$

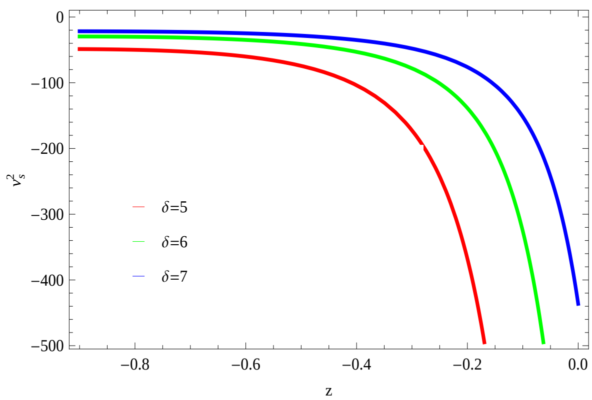

Figure 4.5: Plot of v_s^2 versus z for generalized ghost PDE in DGP framework.

$$
\begin{aligned}
+ & \delta)\Omega_D\dot{H} - 2\beta\epsilon\sqrt{\Omega_{r_c}}\dot{H} + 2(-2+\delta)(\alpha+2\beta H)\dot{\Omega}_D - \epsilon(\alpha+\beta H)\dot{\Omega}_{r_c} \\
/ & \sqrt{\Omega_{r_c}}))/(2(\alpha+\beta H) + 2(-2+\delta)(\alpha+2\beta H)\Omega_D - 2\epsilon(\alpha+\beta H) \\
\times & \sqrt{\Omega_{r_c}})^2))/3(-1+3(1-\Omega_D-2\epsilon(\Omega_{r_c})^{1/2})(\alpha+\beta H)/(2(\delta-2)(\alpha+2 \\
\times & \beta H)\Omega_D - 2\epsilon(\Omega_{r_c})^{1/2}(\alpha+\beta H) + 2(\alpha+\beta H)) - 1/2). \qquad (4.1.9)
\end{aligned}
$$

We can show the plane of state-finder for three different values by plotting a graph between r and s. Hence, Figure 4.4 can corresponds to phantom and quintessence region of DE for all parametric values of δ. For the derivation of squared speed of sound expression to check the stability behavior of this DGP framework, differentiate Eq.(4.1.5) with respect to time then (4.1.5) and this differential form insert in Eq.(2.8.5), we obtain

$$
\begin{aligned}
v_s^2 &= -1 + \frac{(2-\delta)(\alpha+2\beta H)\left(1-\Omega_D-2\epsilon\sqrt{\Omega_{r_c}}\right)}{(\alpha+\beta H)+(-2+\delta)(\alpha+2\beta H)\Omega_D - \epsilon(\alpha+\beta H)\sqrt{\Omega_{r_c}}} \\
&- (H(\alpha+\beta H)(-4\alpha\beta\epsilon^2{\Omega_{r_c}}^{3/2}\dot{H} + 2\sqrt{\Omega_{r_c}}(\alpha\beta\left(-1+\Omega_D\right)\dot{H} + (\alpha \\
&+ 2\beta H)(\alpha(-1+\delta)+\beta(-3+2\delta)H)\dot{\Omega}_D) - 2\epsilon\Omega_{r_c}(\alpha\beta\left(-3+\Omega_D\right)\dot{H} \\
&+ (\alpha+2\beta H)(\alpha(-3+2\delta)+\beta(-7+4\delta)H)\dot{\Omega}_D) + \epsilon(\alpha+2\beta H)((\alpha \\
&+ \beta H) + (\alpha(-3+2\delta)+\beta(-7+4\delta)H)\Omega_D)\dot{\Omega}_{r_c}))(4\Big(\alpha(1+(-2+\delta)
\end{aligned}
$$

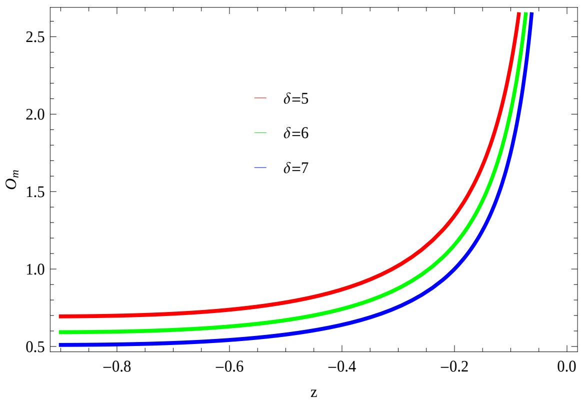

Figure 4.6: Plot of O_m versus z for generalized ghost PDE in DGP framework.

$$\times \quad \Omega_D - \epsilon\sqrt{\Omega_{r_c}})(\alpha + 2\beta H) + \beta H \left(1 + 2(-2+\delta)\Omega_D - \epsilon\sqrt{\Omega_{r_c}}\right)\Bigg)^2$$
$$\times \quad \sqrt{\Omega_{r_c}}\dot{H}). \tag{4.1.10}$$

We can easily exhibit this result in Figure 4.5 which shows that the model is unstable under different values of δ. It can be observed that the $v_s^2 < 0$ for future and present epoch and remains in this direction. Finally, in Figure 4.6, the plot of Om parameter against redshift z in DGP braneworld shows that the trajectories lies in positive direction which tells that the universe transition is in phantom region.

4.2 RS II Braneworld Case

In RS II braneworld model, we chose the flat ($k = 0$) FRW universe as 3-dimension brane fixed in a higher dimensional bulk which is modified field equation is mention above Eq.(2.11.2). In this case, we can be ignored the second term of Eq.(2.11.5) for greater values of L. Moreover, we consider the Tsallis HDE in flat RS II model with the choice of generalized ghost PDE as IR cutoff which is define as $L = (\alpha H + \beta H^2)^{-1}$. For this IR cutoff, the energy density can be obtained

$$\rho_D = \frac{3Bc^2M_p^2(\alpha H + \beta H^2)^{4-2\delta}}{128\pi^2}. \tag{4.2.1}$$

According to Eq.(2.11.2), one can be written in the following form

$$\Omega_m + 2\Omega_D = 1, \tag{4.2.2}$$

where

$$\Omega_D = \frac{Bc^2(\alpha H + \beta H^2)^{4-2\delta}}{16\pi^2}. \tag{4.2.3}$$

We can obtain the differential equation for the Hubble parameter by taking the time derivative of Eq.(2.11.2) and combining with Eqs.(3.1.1), (4.2.1) and (4.2.2), which as follows

$$\frac{\dot{H}}{H^2} = \frac{3(2\Omega_D - 1)(\alpha + \beta H)}{2(\alpha + \beta H) + 2(2\delta - 4)(\alpha + 2\beta)\Omega_D}, \tag{4.2.4}$$

and also have

$$\acute{\Omega}_D = \frac{3\Omega_D(2\Omega_D - 1)((2-\delta)(\alpha + 2\beta H) - (\alpha + \beta H))}{(\alpha + \beta H) + 2(\delta - 2)(\alpha + 2\beta)\Omega_D}. \tag{4.2.5}$$

We derive the EoS parameter of Tsallis HDE on this braneworld scenario from Eq.(1.0.3) with combining the time derivative form of Eq.(4.2.1), which is yield

$$\omega = -1 + \frac{3(2\Omega_D - 1)(\delta - 2)(\alpha + 2\beta H)}{(\alpha + \beta H) + 2(\delta - 2)(\alpha + 2\beta)\Omega_D}. \tag{4.2.6}$$

It can be shown from Figure 4.7 that the EoS parameter exhibits in increases phase and goes towards in phantom region and also remain in this phantom region for all values of δ. Using Eqs.(2.8.3) and (4.2.4), the deceleration parameter q is obtained as

$$q = -1 + \frac{3(2\Omega_D - 1)(\alpha + \beta H)}{2(\alpha + \beta H) + 2(2\delta - 4)(\alpha + 2\beta)\Omega_D}. \tag{4.2.7}$$

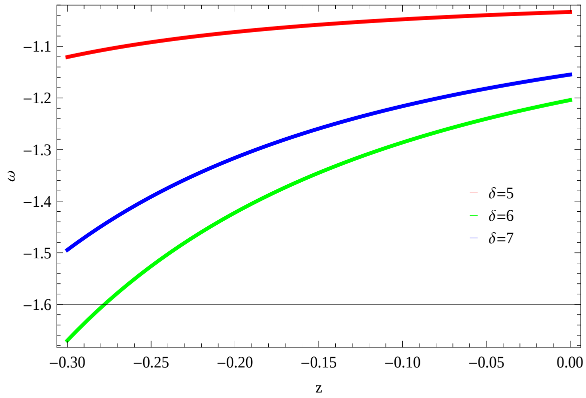

Figure 4.7: Plots of EoS parameters versus z for generalized ghost PDE in RS II braneworld.

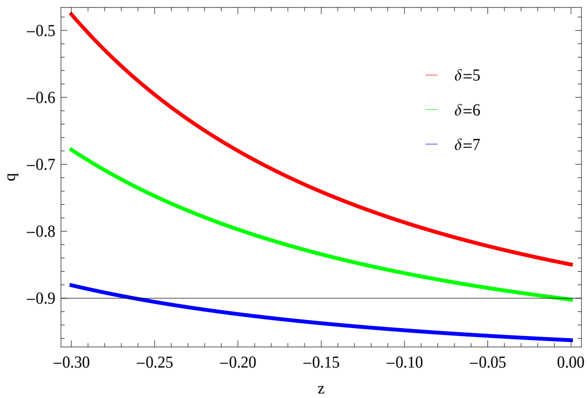

Figure 4.8: Plots of deceleration parameters versus z for generalized ghost PDE in RS II braneworld.

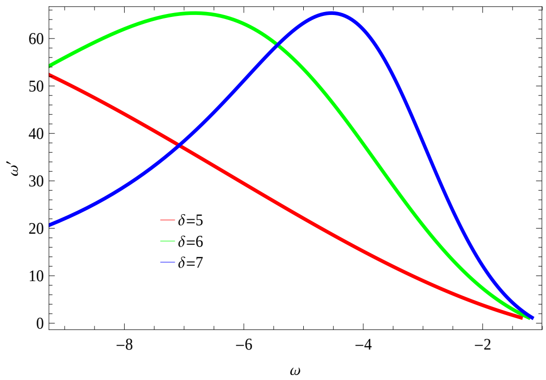

Figure 4.9: Plots of ω' versus ω for generalized ghost PDE in RS II braneworld.

The behavior of q is shown in Figure 4.8. It can be seen that there is a acceleration expansion phase at the latter and present values. In order to find the evolution of EoS, ω' can be written in following form

$$(4.2.8)$$

$$\begin{aligned}\omega' &= (3(\delta-2)(\alpha\beta(-1+2\Omega_D)\dot{H}+2(\alpha+2\beta H)(\alpha(\delta-1)+\beta(3\delta-3)H)\\ &\times \dot{\Omega}_D))/(H(\alpha+\beta H+2(\delta-2)\alpha+2\beta H)\Omega_D)^2. \qquad (4.2.9)\end{aligned}$$

The $\omega'-\omega$ plane for Tsallis HDE with generalized ghost PDE with different values of δ in RS II Scenario is shown in Figure 4.9. For this braneworlds scenario, the $\omega-\omega'$ plane indicates to cosmological CDM region. Also, the approaches meet the thawing phase as well. Using Eqs.(2.8.4), (4.2.7) and double derivative of Eq.(4.2.4) with respect to t, we can find that the state-finders are given as

$$\begin{aligned}r &= 1+(9(\alpha+\beta H)(-1+2\Omega_D))/(2(\alpha+\beta H+2(-2+\delta)(\alpha+2\beta H)\Omega_D))\\ &- (3\alpha\beta(-2+\delta)\Omega_D(-1+2\Omega_D)\dot{H})/(H(\alpha+\beta H+2(-2+\delta)(\alpha+2\beta H)\\ &\times \Omega_D)^2)+2\dot{H}^2/H^4+(3(\alpha+\beta H)(\alpha(-1+\delta)+\beta(-3+2\delta)H)\dot{\Omega}_D)/(H\\ &\times (\alpha+\beta H+2(-2+\delta)(\alpha+2\beta H)\Omega_D)^2), \qquad (4.2.10)\end{aligned}$$

and

$$
\begin{aligned}
s &= 2((9(\alpha+\beta H)(-1+2\Omega_D))/(2(\alpha+\beta H+2(-2+\delta)(\alpha+2\beta H)\Omega_D)) \\
&- (3\alpha\beta(-2+\delta)\Omega_D(-1+2\Omega_D)\dot{H})/(H(\alpha+\beta H+2(-2+\delta)(\alpha+2\beta H) \\
&\times \Omega_D)^2)+2\dot{H}^2/H^4+(3(\alpha+\beta H)(\alpha(-1+\delta)+\beta(-3+2\delta)H)\dot{\Omega}_D)/(H \\
&\times (\alpha+\beta H+2(-2+\delta)(\alpha+2\beta H)\Omega_D)^2))(9(-1+((\alpha+\beta H)(1-2\Omega_D)) \\
&/ (\alpha+\beta H+2(-2+\delta)(\alpha+2\beta H)\Omega_D)))^{-1}. \qquad (4.2.11)
\end{aligned}
$$

The evolution of the state-finder parameters for generalized ghost PDE in the framework of RS II braneworld have been plotted in Figure 4.10. From this figure we can see that, it corresponds to chaplygin gas.
We can derive the explicit result of v_s^2 for Tsallis HDE in RS II braneworld from result (2.8.5), which is

$$
\begin{aligned}
v_s^2 &= (3H(\alpha+\beta H)(\alpha\beta(1-2\Omega_D)\dot{H}-2(\alpha+2\beta H)(\alpha(-1+\delta)+\beta(-3 \\
&+ 2\delta)H)\dot{\Omega}_D))/(2(\alpha+2\beta H)((\alpha+\beta H)+2(-2+\delta)(\alpha+2\beta H)\Omega_D)^2\dot{H}) \\
&- 1+(3(-2+\delta)(\alpha+2\beta H)(-1+2\Omega_D))/((\alpha+\beta H)+2(-2+\delta)(\alpha \\
&+ 2\beta H)\Omega_D). \qquad (4.2.12)
\end{aligned}
$$

We can be depicted this result in Figure 4.11. Here clearly we see that, squared speed of sound is ever positive showing that Tsallis HDE in RS II framework is always stable against z. It is helpful to note that, depending on the all values of δ, Tsallis HDE in RSII framework can cover the stability condition.

The behavior of Om diagnostic can be checked in Figure 4.12 for RS II braneworld. We can see that in future and present epoch the trajectories always corresponds phantom phase of the universe.

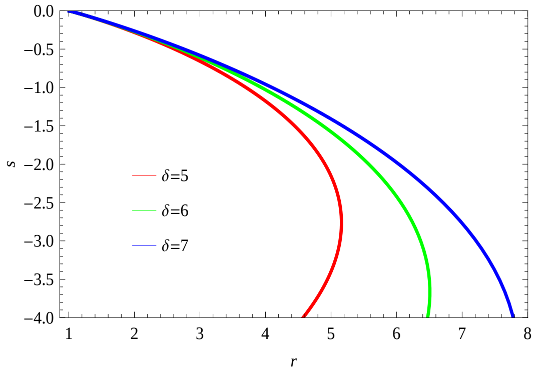

Figure 4.10: Plots of state-finder parameters s versus r for generalized ghost PDE in RS II braneworld.

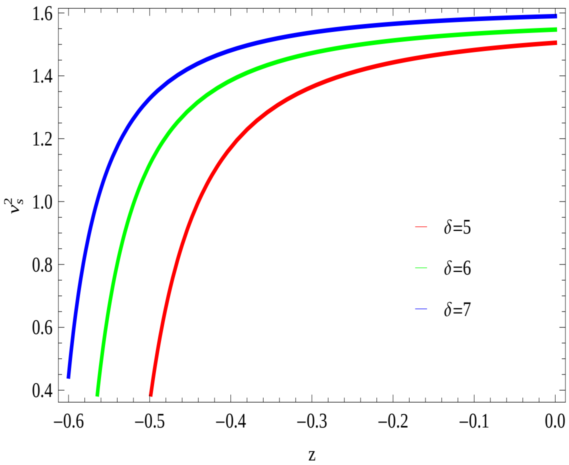

Figure 4.11: Plot of v_s^2 versus z for generalized ghost PDE in RS II braneworld.

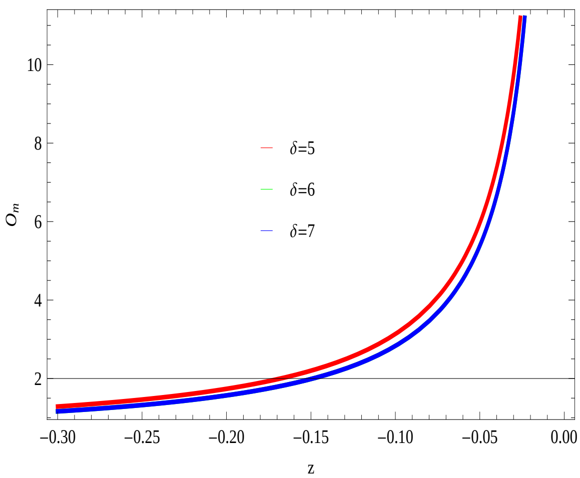

Figure 4.12: Plot of O_m versus z for generalized ghost PDE in RS II braneworld.

Chapter 5
Tsallis Holographic Dark Energy in Dynamical Chern-Simons Modified Gravity

In this chapter, we use Tsallis holographic dark energy model with generalized ghost pilgrim dark energy as infra-red cutoff in the dynamical Chern-Simons theory in the flat FRW universe. In this direction, we study some cosmological parameters like equation of state, deceleration parameter, squared sound speed and Om parameter. We also establish some cosmic planes such as $\omega - \omega'$ and $r - s$ on the basis of presents day observational data.

5.1 Dynamical Chern-Simons Modified Gravity Case

In case of dynamical theory of CS gravity, modified Friedmann equation is written above in Eq.(2.12.5). Using Eq.(3.1.3), one can we rewrite Eq.(2.12.5) as

$$1 = \Omega_m + \Omega_D + \frac{b^2 a^{-6}}{6H^2}. \tag{5.1.1}$$

Hubble parameter is calculated by taking time derivative of Eq.(2.12.8) and then numerically solving with Eqs.(1.0.3), (3.1.2) and (5.1.1) we have

$$\frac{\dot{H}}{H^2} = \frac{-3\left(1 - \Omega_D + \frac{b^2 a^{-6}}{6H^2}\right)(\alpha + \beta H)}{2(2-\delta)(\alpha + 2\beta H)\Omega_D + 2(\alpha + \beta H)}, \tag{5.1.2}$$

and evolutionary equation

$$\Omega'_D = \frac{-3\Omega_D\left(1 - \Omega_D + \frac{b^2 a^{-6}}{6H^2}\right)((2-\delta)(\alpha + 2\beta H) - (\alpha + \beta H))}{(2-\delta)(\alpha + 2\beta H)\Omega_D + (\alpha + \beta H)}. \tag{5.1.3}$$

For the calculation of EoS and deceleration parameters, we obtain the equations as

$$\omega = -1 + \frac{(2-\delta)\left(1 - \Omega_D + \frac{b^2 a^{-6}}{6H^2}\right)(\alpha + 2\beta H)}{(2-\delta)(\alpha + 2\beta H)\Omega_D + (\alpha + \beta H)}, \tag{5.1.4}$$

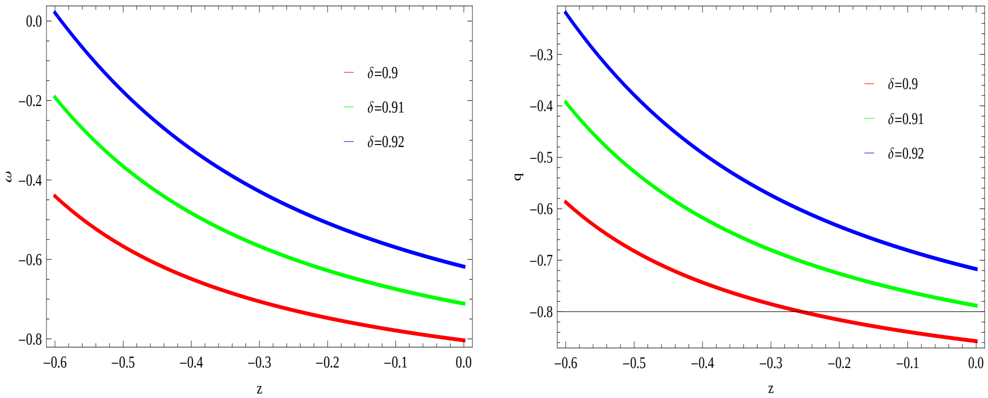

Figure 5.1: Plots of EoS and deceleration parameters versus z for generalized ghost PDE in CS modified gravity.

and

$$q=-1+\frac{3\left(1-\Omega_D+\frac{b^2a^{-6}}{6H^2}\right)(\alpha+\beta H)}{2(2-\delta)(\alpha+2\beta H)\Omega_D+2(\alpha+\beta H)}. \tag{5.1.5}$$

The plot of EoS parameter ω and deceleration parameter q versus z for CS gravity is shown in Figure 5.1. It can be observed that the range of ω remains in the quintessence phase of the universe at the future and present epoch. The trajectories of q describes accelerated expansion phase of the universe. The ω' is obtain from Eq.(5.1.4) which is given as

$$\begin{aligned}
\omega' &= (2\beta(2-\delta)(1+b^2/6a^6H^2-\Omega_D)\dot{H})/(H(\alpha+\beta H)+(2-\delta)(\alpha+2\beta H)\\
&\times \Omega_D)+((2-\delta)(\alpha+2\beta H)(-b^2/a^6H-b^2\dot{H}/3a^6H^3-\dot{\Omega}_D))/(H(\alpha+\beta\\
&\times H)+(2-\delta)(\alpha+2\beta H)\Omega_D)-((2-\delta)(\alpha+2\beta H)(1+b^2/6a^6H^2\\
&- \Omega_D)(\beta\dot{H}+2\beta(2-\delta)\Omega_D\dot{H}+(2-\delta)(\alpha+2\beta H)\dot{\Omega}_D))/((\alpha+\beta H)\\
&+ (2-\delta)(\alpha+2\beta H)\Omega_D)^2. \qquad (5.1.6)
\end{aligned}$$

The $\omega-\omega'$ plane for CS modified gravity is described in Figure 5.2. In this plane, we can see that $\omega'>0$ and $\omega<0$ rest in thawing region. In this theory, the state-finder parameters calculation leads to

$$r = 1-(9(\alpha+\beta H)(1+(b^2)/(6a^6H^2)-\Omega_D))/(2((\alpha+\beta H)-(-2+\delta)(\alpha$$

$$
\begin{aligned}
+ &\quad 2\beta H)\Omega_D)) + (1/4H)(-(6\beta(1+b^2/(6a^6H^2)-\Omega_D)\dot{H})/((\alpha+\beta H)-(\\
- &\quad 2+\delta)(\alpha+2\beta H)\Omega_D) + (8\dot{H}^2)/(H^3) + (2(\alpha+\beta H)(b^2(3H^2a+a\dot{H}) \\
+ &\quad 3a^7H^3\dot{\Omega}_D))/(a^7H^3((\alpha+\beta H)-(-2+\delta)(\alpha+2\beta H)\Omega_D)) + (3(\alpha+\beta \\
\times &\quad H)(1+b^2/(6a^6H^2)-\Omega_D)(2\beta(1-2(-2+\delta)\Omega_D)\dot{H}-2(-2+\delta)(\alpha \\
+ &\quad 2\beta H)\dot{\Omega}_D))/((\alpha+\beta H)-(-2+\delta)(\alpha+2\beta H)\Omega_D)^2), \qquad (5.1.7)
\end{aligned}
$$

and,

$$
\begin{aligned}
s &= (9(-1+((\alpha+H\beta)(1+(b^2/6a^6H^2)-\Omega_D))/(\alpha+H\beta-(\alpha+2H\beta)(\\
- &\quad 2+\delta)\Omega_D))^2)^{-1}(-(9(\alpha+H\beta)(1+(b^2/6a^6H^2)-\Omega_D))/(2(\alpha+H\beta \\
- &\quad (\alpha+2H\beta)(-2+\delta)\Omega_D)) + (1/4H)(-(6\beta(1+(b^2/6a^6H^2)-\Omega_D)\dot{H}) \\
/ &\quad (\alpha+H\beta-(\alpha+2H\beta)(-2+\delta)\Omega_D) + (8\dot{H}^2/H^3) + (2(\alpha+H\beta)(ab^2(\\
\times &\quad 3H^2+\dot{H}) + 3a^7H^3\dot{\Omega}_D))/(a^7H^3(\alpha+H\beta-(\alpha+2H\beta)(-2+\delta)\Omega_D)) \\
+ &\quad 3(\alpha+H\beta)(1+(b^2/6a^6H^2)-\Omega_D)(2\beta(1-2(-2+\delta)\Omega_D)\dot{H}-2(\alpha \\
+ &\quad 2H\beta)(-2+\delta)\dot{\Omega}_D)(\alpha+H\beta-(\alpha+2H\beta)(-2+\delta)\Omega_D)^2)). \qquad (5.1.8)
\end{aligned}
$$

The Figure 5.3, show the graph for state-finder parameters of CS modified gravity in Tsallis HDE model. It observe that $s < 0$ and $r > 1$ which represents the chaplygin gas of the universe for all values of δ. For squared sound speed expression in this manner, we take the time derivative of Eq.(5.1.4) and after some numerically calculations we get

$$
\begin{aligned}
v_s^2 &= ((2-\delta)(2(\alpha+2\beta H)^2(1+b^2/6a^6H^2-\Omega_D)((\alpha+\beta H)-(-2+\delta)(\alpha \\
+ &\quad 2\beta H)\Omega_D) - 1/((-2+\delta)\dot{H})H(\alpha+\beta H)(b^2(\alpha+2\beta H)((-\alpha-\beta H) \\
+ &\quad (-2+\delta)(\alpha+2\beta H)\Omega_D)(a^6H)^{-1} - \alpha\beta(-1+\Omega_D)\dot{H} + (\alpha+2\beta H)(\alpha(\\
- &\quad 3+\delta) + \beta(-5+2\delta)H)\dot{\Omega}_D + 1/(6a^6H^3)b^2((-2\alpha^2-\beta H(5\alpha+4\beta H) \\
+ &\quad 2(-2+\delta)(\alpha+2\beta H)^2\Omega_D)\dot{H} + (-2+\delta)H(\alpha+2\beta H)^2\dot{\Omega}_D))))/(2(\alpha
\end{aligned}
$$

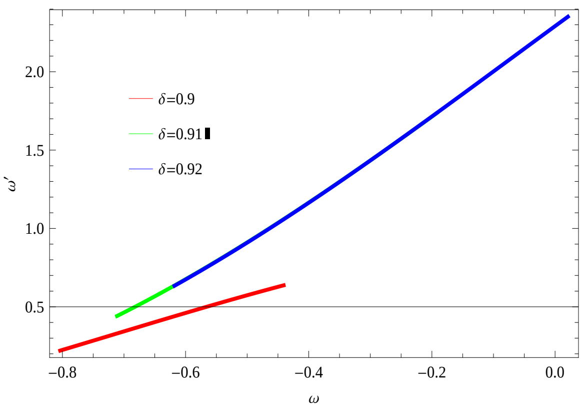

Figure 5.2: Plots of ω' versus ω for generalized ghost PDE in CS modified gravity.

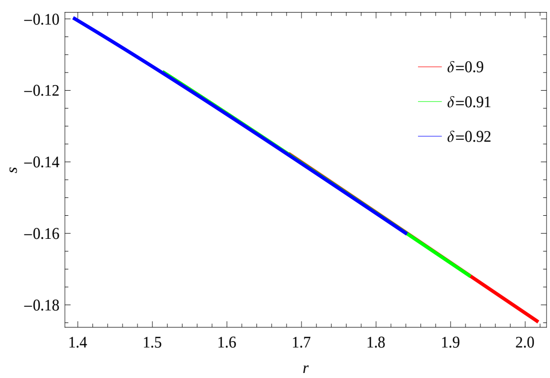

Figure 5.3: Plots of state-finder parameters s versus r for generalized ghost PDE in CS modified gravity.

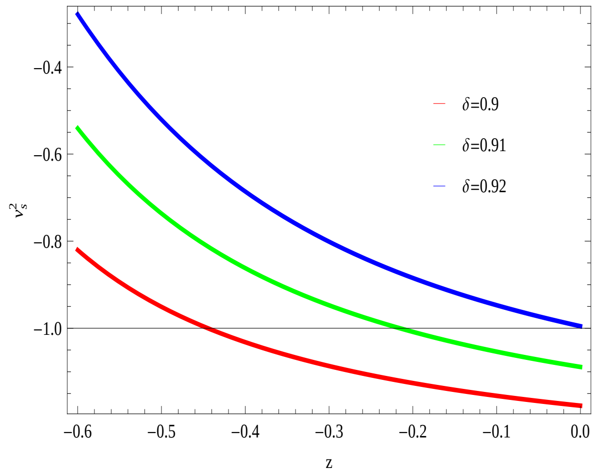

Figure 5.4: Plot of v_s^2 versus z for generalized ghost PDE in CS modified gravity.

$$+ \quad 2\beta H)(\alpha + \beta H - (-2+\delta)(\alpha + 2\beta H)\Omega_D)^2). \tag{5.1.9}$$

We have described the range of squared sound of speed v_s^2 with respect to the redshift parameter z in Figure 5.4. From the figure, we have seen that for generalized ghost PDE in CS gravity the v_s^2 lies in negative and less than 0 through out cosmic evolution which exhibits the instability of our model. Also, we can check the era of the universe throughout Om parameter for CS modified gravity. From Figure 5.5, it can be observed that the trajectories of Om parameter lies in negative phase at latter and present epoch which describes the quintessence region of the universe.

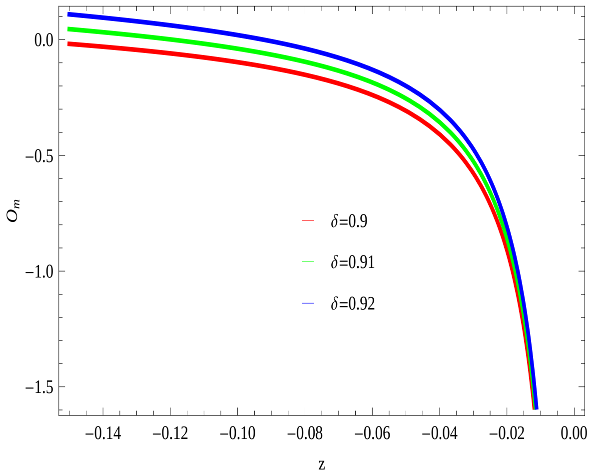

Figure 5.5: Plot of O_m versus z for generalized ghost PDE in CS modified gravity.

Chapter 6
Summary

Our work is based on the motivation of the flat universe. By the help of HDE models, different results and constraints have been investigated on $\Omega_{k=0}$. Nowadays, many researcher interested in flat universe to study acceleration of the universe with the help of cosmological parameters. In order to find the best-fit model to discuss DE phenomenon, there are two directions that are dynamical DE models and modified theories of gravity. One of the dynamical model is HDE which is also modified in different forms such as generalized, Tsallis, Renyi and Sharma-Mittal HDE models, etc. The modified theories include $f(R)$ theory, $f(T)$ theory, fractal cosmology, DGP braneworld, LQC, dynamical CS gravity, RS II braneworld, etc.

In our work, chapter $2-4$ deal with the investigation of different cosmological consequences by taking modified Tsallis HDE with generalized ghost PDE as a IR cutoff in the flat scenario of the universe. Moreover, the other direction which we have used is a modified theories of gravity such as Cyclic universe, DGP braneworld, RS II braneworld and dynamical CS modified gravity theory. We focuss our attentions to evaluate the EoS parameter, deceleration parameter, $\omega-\omega'$ analysis, $r-s$ state-finder parameter, v_s^2 (squared speed of sound) and O_m diagnostic. Expressions of all these models with constant parametric values have been plotted in figures with redshift parameter z.

We have studied the trajectories behavior of EoS parameter versus z redshift parameter by plotting in figures. In Figure 3.1, we check the behavior of EoS parameter as a function of redshift z for three different values of δ including the values $\delta=5,6,7$. Here we observed that, for increasing value of z the evolution $\omega(z)$ tend to lower negative values. At the present time where $\omega(z) = 0$, it remain in phantom period. Hence, It can be observed that for Tsallis HDE in the cyclic universe, the evolutionary ω starts from ΛCDM regime and moved in phantom region. In DGP braneworld model, we have seen that $\omega(z)$ is closer to ΛCDM period of the universe and then always remain in phantom era. Moreover, in the investigation of RS II braneworld scenario, the evolutionary EoS parameter exhibits in increases phase and goes towards in phantom region and also remain in this phantom region for all values of δ. But in case of dynamical CS modified gravity, the range of ω remains in the quintessence phase of the universe at the latter and present epoch with the parametric values $\delta = 0.9, 0.91, 0.92$.

The trajectories of deceleration paramete q has been discussed in figures by plotting its results versus redshift z. In the cyclic universe scenario, We observed that for increased of redshift z, the deceleration parameter is increasing and increases to lesser negative values. Thus, it can be seen that the transition of the universe shows in accelerating phase. It is obvious that the model in DGP and RS II braneworld scenario can cover the accelerating phase of the universe. Also in the investigation of dynamical CS modified gravity, the trajectories of q describes accelerated expansion phase of the universe.

We have constructed the trajectories of planes $\omega - \omega'$ and $r - s$ statefinder. The evolution of $\omega - \omega'$ can be observed that the values of ω' is increases as increases the values of ω. Hence, in the framework of cyclic, RS II and dynamical CS modified gravity, all models can be shown that that the $\omega' > 0$ and $\omega < 0$ which indicates the thawing region of the universe. However, in DGP braneworld, the trajectories shows that $\omega' > 0$ and $\omega < 0$ which covers the freezing phase of the universe. It can be observed that the graphs of these models shows chaplygin gas because here $r > 1$ and $s < 0$. We also investigate the state-finder parameter for this DGP braneworld by plotting in Figure 4.4, it corresponds to phantom and quintessence region of DE for all parametric values of δ.

The squared speed of sound help to check the stability behavior of these modified gravity theories for THDE model, we have used different parametric values of δ. According to δ, in the framework of the cyclic and RS II scenario, at present and latter epoch one can see that the graph shows $v_s^2 > 0$. Hence, the behavior of these models have shown stability. But in case of other theories DGP and dynamical CS, the model is unstable having negative values ($v_s^2 < 0$).

Also, we have explored the Om diagnostic for all models of modified theories of gravity to describe different phases of the universe. We plot these parametric results for different values of constant δ against z redshift. The Om trajectories covers the negative values in the scenario of cyclic universe and dynamical CS gravity which corresponds to quintessence behavior of the universe. Although, in the investigation of DGP and RS II braneworld the trajectories remain in the direction of positive values which tells that the universe transition is in the phantom region.

Chapter 7
References

[1] A. G. Riess et al., Astron. J. **116**, 1009-1038 (1998).

[2] S. Perlmutter et al., Astrophys. J. **517**, 565-586 (1999).

[3] P. de Bernardis et al., Nature **404**, 955-959 (2000).

[4] S. Perlmutter et al., Astrophys. J. **598**, 102 (2003).

[5] S. Hanany et al., Astrophys. J. **545**, L5 (2000).

[6] C. B. Netterfield et al., Astrophys. J. **571**, 604-614 (2000).

[7] D. N. Spergel et al., Astrophys. J. Suppl. **148**, 175-194 (2003).

[8] M. Colless et al., Mon. Not. R. Astron. Soc. **328**, 1039 (2001).

[9] M. Tegmark et al., Phys. Rev. D**69**, 103501 (2004).

[10] S. Cole et al., Mon. Not. R. Astron. Soc. **362**, 505 (2005).

[11] V. Springel, C. S. Frenk and S. M. D. White (2006), Nature **440**, 1137.

[12] M. Roos, Introduction to cosmology (John Wiley and Sons, UK) (2003).

[13] P. J. E. Peebles and B. Ratra, Rev. Mod. Phys. **75**, 559-606 (2003).

[14] J. Kratochvil, A. Linde, E. V. Linder and M. Shmakova, JCAP **0407**, 001 (2004).

[15] C. Wetterich, symmetry, Nucl. Phys. B **302**, 668-696 (1988).

[16] B. Ratra, J. Peebles, Phys. Rev. D **37**, 3406 (1988).

[17] R. R. Caldwell, Phys. Lett. B **545**, 23-29 (2002).

[18] R. R. Caldwell, M. Kamionkowski and N. N. Weinberg, Phys. Rev. Lett. **91**, 071301 (2003).

[19] T. Chiba, T. Okabe and M. Yamaguchi, Phys. Rev. D **62**, 023511 (2000).

[20] C. Armendariz-Picon, V. F. Mukhanov and P. J. Steinhardt, Phys. Rev. Lett. **85**, 4438 (2000).

[21] C. Armendariz-Picon, V. F. Mukhanov and P. J. Steinhardt, Phys. Rev. D **63**, 103510 (2001).

[22] A. Y. Kamenshchik, U. Moschella and V. Pasquier, Phys. Lett. B **511**, 265-268 (2001).

[23] M. C. Bento, O. Bertolami and A. A. Sen, Phys. Rev. D **66**, 043507 (2002).

[24] R. G. Cai, Phys. Lett. B **657**, 228-231 (2007).

[25] H. Wei and R. G. Cai, Phys. Lett. B **660**, 113 (2008).

[26] K. Y. Kim, H. W. Lee and Y. S. Myung, Phys. Lett. B**660**, 118 (2008).

[27] K. Koyama, Class. Quant. Gravity **24**, R 231-R253 (2007).

[28] R. C. Tolman, Phys. Rev. **38** 1758 (1931).

[29] R. Lazkozet, R. Maarens and E. Majerotto, Phys. Rev. D **74**, 083510 (2006).

[30] L. Randall and R. Sundrum, Phys. Rev. Lett. **83**, 4690 (1999).

[31] J. Garriga and T. Tanaka, Phys. Rev. Lett. **84**, 2778 (2000).

[32] T. Wiseman, Phys. Rev. D **65**, 124007 (2002).

[33] I. Giannakis and H. c. Ren, Phys. Rev. D **63**, 024001 (2001).

[34] H. Kudoh and T. Tanaka, Phys. Rev. D **64**, 084022 (2001).

[35] R. C. Tolman, Phys. Rev. **38**, 1758 (1931).

[36] J. Khoury, B. A. Ovrut, P. J. Steinhardt and N. Turok, Phys. Rev. D **64**, 123522 (2000).

[37] P. J. Steinhardt and N. Turok, Science **296**, 1436 (2002).

[38] P. J. Steinhardt and N. Turok, Phys. Rev. D **65**, 126003 (2002).

[39] L. A. Boyle, P. J. Steinhardt and N. Turok, Phys. Rev. D **70**, 023504 (2004).

[40] P. J. Steinhardt and N. Turok, Science **312**, 1180 (2006).

[41] M. G. Brown, K. Freese and W. H. Kinney, JCAP **0803**, 002 (2008).

[42] L. Baum and P. H. Frampton, Phys. Rev. Lett. **98**, 071301(2007).

[43] X. Zhang, Eur. Phys. J. C **60**, 661 (2009).

[44] R. Caldwell, Phys. Lett. B **545**, 23 (2002).

[45] R. R. Caldwell, M. kamionkowski and N. N. Weinberg, Phys. Rev. lett. **91**, 071301 (2003).

[46] A. Ashtekar, T. Pawlowski and P. Singh, Phys. Rev. D **74**, 084003 (2006).

[47] T. L. Smith, A. L. Erickcek, R. R. Caldwell and M. Kamionkowski, Phys. Rev. D **77**, 024015(2008).

[48] A. Lue, L.M. Wang and M. Kamionkowski, Phys. Rev. Lett. **83**, 1506 (1999).

[49] R. Jackiw, Phys. Rev. D **68**, 104012 (2003).

[50] S. Alexander and N. Yunes, Phys. Rep. **480**, 155 (2009).

[51] T. L. Smith et al., Phys. Rev. D **77**, 024015 (2008).

[52] S. H. S. Alexander, S. J. J. Gates, J. Cosmol. Astropart. Phys. **0606**, 18 (2006).

[53] B. A. Campbell et al., Nucl. Phys. B **399**, 137 (1993).

[54] S. Alexander and N. Yunes, Phys. Rep. **480**, 1 (2009).

[55] Y. S. Myung, Eur. Phys. J. C **73**, 2515 (2013).

[56] J. G. Silva and A. F. Santos, Eur. Phys. J. C **73**, 2500 (2013).

[57] A. Jawad and A. Sohail, Astrophys. Space Sci. **359**, 55 (2015).

[58] G. 't Hooft, [arXiv:hep-th/0003004] (2000).

[59] A. Cohen, D. Kaplan and A. Nelson, Phys. Rev. Lett. **82**, 4971 (1999).

[60] J. D. Bekenstein, Lett. al Nuovo Cim. **4**(15), 737 (1972).

[61] J. D. Bekenstein, Phys. Rev. D **7**, 2333 (1973).

[62] J. D. Bekenstein, Phys. Rev. D **9**, 3292 (1974).

[63] S. W. Hawking, Nature **248**, 30-31 (1974).

[64] G. 't Hooft, Conf. Proc. C **930308**, 284-296 (1993).

[65] P. Horava and D. Minic, Phys. Rev. Lett. **85**, 1610 (2000).

[66] M. Li, Phys. Lett. B **603**, 1 (2004).

[67] S. D. H. Hsu, Phys. Lett. B **594**, 13 (2004).

[68] C. Tsallis and L. J. L. Cirto, Eur. Phys. J. C **73**, 2487 (2013).

[69] B. Guberina, R. Horvat and H. Nikoli, J. Cosmol. Astropart. Phys. **01**, 012 (2007).

[70] S. Ghaffari, M. H. Dehghani and A. Sheykhi, Phys. Rev. D **89**, 123009 (2014).

[71] A. Sayahian Jahromi, et al., Phys. Lett. B **780**, 21 (2018).

[72] J. Dutta, S. Chakraborty and M. Ansari, Modern Phys. Lett. A **25**, 3069 (2010).

[73] D. J. Liu, H. Wang and B. Yang, Phys. Lett. B **694**, 6 (2010).

[74] A. Sheykhi, M. H. Dehghani and S. Ghaffari, Internat. J. Modern Phys. D **25**, 1650018 (2016).

[75] S. Ghaffari, A. Sheykhi and M. H. Dehghani, Phys. Rev. D **89**, 123009 (2014).

[76] T. Bandyopadhyay, Internat. J. Theoret. Phys. **50**, 3 (2011).

[77] E. N. Saridakis, Phys. Lett. B **660**, 138 (2008).

[78] J. Zhang, X. Zhang and H. Liu, Eur. Phys. J. C **52**, 693 (2007).

[79] A. Sheykhi, M. Tavayef and H. Moradpour, Can. J. Phys. **96** (9), 1034 (2018).

[80] A. Jawad, K. Bamba, M. Younas, S. Qummer and S. Rani, Symmetry **10**, 635 (2018).

[81] S. Ghaffari, H. Moradpour, V. B. Bezerra, J. P. Morais Graca and I.P. Lobo, Phys.Dark Univ. **23**, 100246 (2019).

[82] A. Ashtekar, T. Pawlowski and P. Singh, Phys. Rev. D **73**, 124038 (2006).

[83] A. Ashtekar, T. Pawlowski and P. Singh, Phys. Rev. D **74**, 084003 (2006).

[84] A. Ashtekar, AIP Conf. Proc. **861**, 3 (2006).

[85] P. Singh, K. Vandersloot, G. SV. Vereshchagin, Phys. Rev. D **74**, 043510 (2006).

[86] C. Roveli, Living Rev. Rel. **1**, 1 (1998).

[87] A. Ashtekar and J. Lewandowski, Class. Quant. Grav. **21**, 53 (2000).

[88] M. Bojowad, Living Rev. Rel. **8** 11 (2005).

[89] A. Ashtekar, M. Bojowad and J. Lewandowski, Adv. Theor. Math. Phys. **7**, 233 (2003).

[90] A. Ashtekar, AIP Conf. Proc. **861**, 3 (2006).

[91] C. Rovelli, Quantum Gravity, Cambridge University Press, Cambridge (2004).

[92] M. Jamil and U. Debnath, Astrophys Space Sci. **333**, 3 (2011).

[93] E. M. Barboza Jr, R. C. Nunes, E. M. C. Abreu and J. A. Neto, Physica A **36**,301 (2015).

[94] R. C. Nunes, et al., J. Cosmol. Astropart. Phys. **08**, 051 (2016).

[95] E. N. Saridakis, Phys. Lett. B **660**, 138 (2008).

[96] Q. G. Huang and M. Li, J. Cosmol. Astropart. Phys. **04**, 013 (2004).

[97] P. J. E. Peebles and B. Ratra, Rev. Mod. Phys. **75**, 559-606 (2003).

[98] J. Kratochvil, A. Linde, E. V. Linder and M. Shmakova, JCAP **0407**, 001 (2014).

[99] G. t' Hooft and L. Susskind, J. Math. Phys. **36**, 6377 (1995).

[100] A. Cohen, D. Kaplan and A. Nelson, Phys. Rev. Lett. **82**, 4971 (1999).

[101] C. Tsallis, J. Statist. Phys. **52**, 479 (1988).

[102] M. L. Lyra and C. Tsallis, Phys. Rev. Lett. **80**, 53 (1998).

[103] C. Tsallis, R. S. Mendes and A. R. Plastino, Physica A **261**, 534 (1998).

[104] G. Wilk and Z. Wlodarczyk, Phys. Rev. Lett. **84**, 2770 (2000).

[105] C. Tsallis and L. J. L. Cirto, Eur. Phys. J. C **73**, 2487 (2013).

[106] S. Wang, Y. Wang and M. Li, Phys. Rept. **696**, 1 (2017).

[107] H. Wei, Class. Quantum Grav. **29**, 175008 (2012).

[108] E. Babichev, V. Dokuchev and Y. Eroshenko, Phys. Rev. Lett. **93**, 021102 (2004).

[109] E. Babichev, V. I. Dokuchev and Y. N. Eroshenko, J. Exp. Theor. Phys. **100**, 528 (2005).

[110] F. R. Urban and A. R. Zhitnitsky, Phys. Rev. D **80**, 063001 (2009).

[111] F. R. Urban and A. R. Zhitnitsky, JCAP **09**, 018 (2009).

[112] F. R. Urban and A. R. Zhitnitsky, Phys. Lett. B **688**, 9 (2010).

[113] F. R. Urban and A. R. Zhitnitsky, Nucl. Phys. B **835**, 135 (2010).

[114] F. R. Urban and A. R. Zhitnitsky, Phys. Lett. B **695**, 41 (2011).

[115] E. Ebrahimi and A. Sheykhi, Phys. Lett. B **706**, 19 (2011).

[116] A. Sheykhi and A. Bagheri, Europhys. Lett. **95**, 39001 (2011).

[117] A. Sheykhi, M. M. Sadegh, Gen. Relativ. Gravit. **44**, 449 (2012)

[118] A. Rozas-Fernandez, Phys. Lett. B **709**, 313 (2012).

[119] K. Karami and K. Fahimi, Class. Quantum Grav. **30**, 065018 (2013).

[120] A. R. Zhitnitsky, Phys. Rev. D **86**, 045026 (2012).

[121] R. G. Cai et al., Phys. Rev. D **86**, 023511 (2012).

[122] M. Malekjani, Int. J. Mod. Phys D **22**, 1350084 (2013)

[123] K. Karami and K. Fahimi, Class. Quantum Grav. **30**, 065018 (2013).

[124] K. Karami et al., Int. J. Mod. Phys. D **22**, 1350018 (2013).

[125] M. Sharif and A. Jawad, Astrophy. Space Sci. **351**, 321 (2014).

[126] R. R. Caldwell and E. V. Linder, Phys. Rev. Lett. **95**, 141301 (2005).

[127] V. Sahni, T. D. Saini, A. A. Starobinsky and U. Alam, JETP Lett. **77**, 201 (2003).